

MASTER THESIS , JANUARY 2013

# Development and Fabrication of a Microfluidic Device for Future Applications in Cell Injection Experiments.

---

Susanne Norlén



**LUNDS UNIVERSITET**  
Lunds Tekniska Högskola

**Supervisors: Henrik Persson<sup>1</sup>, Truls Löwgren<sup>2</sup> & Jonas Tegenfeldt<sup>1,3</sup>**

1. Division of Solid State Physics, Lund University
2. QuNano AB
3. Department of Physics, University of Gothenburg

April 2, 2013

## Abstract

Injection of molecules into cells is used in life sciences and biology today to study cell response to certain substances. Delivery of controlled amounts is important for single cell injection experiments and furthermore, the technique needs to be noninvasive which can be difficult with today's micropipettes. The growing field of nanotechnology has interested many researchers for this purpose and several groups are focusing on developing injection tools with dimensions at the nanoscale. So far the developed techniques have been limited either to single injections or by the slow process of diffusion which both are barriers that needs to be overcome in this area. Our solution is to develop a microfluidic device with hollow nanowires (HNWs) that has the ability to inject molecules into cells with a pressure driven flow, since this could allow fast and repeated injection of substances. Therefore, a microfluidic system has been created, as a first step in the development of such a device. The channel walls are made of atomic layer deposited  $\text{Al}_2\text{O}_3$  and supported by a cured benzocyclobutene based resin. The fabrication of the channels has been realized by etching down microstructures in an epitaxially grown InAs substrate. The fact that the fabrication starts from a III-V substrate opens up the possibility to integrate semiconductor nanowires (NWs) in the process, since they can be epitaxially grown on III-V substrates. The wires can be used as templates for creating injection needles with nanodimensions. The functionality of the channels has been proven in fluidic tests where a fluorescent dye was injected with an applied pressure of around 50 mbar. In future devices, where nanowires are connected to the channels, cells could be cultured on top of the wires and substances introduced through the fluidic system to reach the cells. This results in faster injection than similar devices that rely on diffusion, with a method that allows for repeated and controlled injection of molecules.

## Sammanfattning på svenska

Det här projektet har bestått av att utveckla en del av en mikrofluidik-komponent vars användningsområde är att injicera molekyler i celler. Den fullständiga komponenten är baserad på ett kanalsystem som är anslutet till ihåliga nanotuber, där tuberna kommer att fungera som injektionsnålar. Kanalsystemet i sin tur kan kopplas till makroskopiska tryckpumpar så att injiceringen kan utföras med datorkontroll.

Flera forskargrupper har redan skapat injektionsverktyg på nanoskalan, men hittills har de varit begränsade till experiment där upprepad injicering inte har varit möjligt eller injicering där molekylerna diffunderat genom tuberna in i cellerna, vilket är ett långsamt förlopp. Förhoppningen är att denna komponent istället ska klara av att injicera molekyler in i celler med tryckdrivet flöde och kanalsystemet kommer göra det möjligt att byta vätska samt att utföra upprepad injektion in i samma cell.

Syftet med det här projektet var att utveckla själva kanalsystemet och testa dess funktion. Målet var ett skapa kanalerna genom att utgå från ett III-V substrat, då det öppnar upp för möjligheten att integrera nanotrådar av samma material i processen, eftersom dessa kan växas med epitaxi på III-V filmer. Genom att använda nanotrådarna som mall i fortsatt fabrikation så kan man skapa ihåliga nanotuber som är direkt anslutna till kanalen under. Kanalerna har tillverkats i aluminiumoxid och i fluidik-testerna har fluorescerande molekyler blandade med etanol injicerats genom dessa och filmats i mikroskop.

Projektet har utförts på avdelningen för Fasta Tillståndets Fysik, Lunds Tekniska Högskola, och i samarbete med företaget QuNano AB. I projektet har modellering, tillverkning och fluidik-tester av komponenten ingått. Resultaten har sedan använts av QuNano AB för utvecklandet av en ny, förbättrad design för komponenten.

## Acknowledgements

I would like to start by thanking my supervisors **Truls Löwgren** and **Henrik Persson** for all their help, support and encouragement during this project, it has been really great working with the two of you! **Mikael Björk**, who has been highly involved with this project, also deserves the greatest thanks for all his input and for developing the designs. I also want to thank **Jonas Tegenfeldt** for his contributions and especially the opportunity to carry out this project within his group and the division of Solid State Physics, I am really grateful.

I want to thank you, **Cassandra Niman**, for the help with COMSOL modeling and all the help in the bio-labs. I want to thank **Christelle Prinz**, **Stina Oredsson** and **Gaëlle Offranc-Piret** for their valuable discussions of applications for the device and other bio related issues. Lastly I would like to thank all other people at **QuNano AB** and at the **Solid State Physics** for all help these months and for making this project as fun as it was!

## Abbreviations

<b>AE</b>	Auger Electrons
<b>ALD</b>	Atomic Layer Deposition
<b>BCB</b>	Benzocyclobutene
<b>BSE</b>	Backscattered Electrons
<b>CVD</b>	Chemical Vapor Deposition
<b>EBL</b>	Electron Beam Lithography
<b>HNW</b>	Hollow Nanowire
<b>ICP</b>	Inductively Coupled Plasma
<b>MOVPE</b>	Metal Organic Vapor Phase Epitaxy
<b>NW</b>	Nanowire
<b>OM</b>	Optical Microscope
<b>PDMS</b>	Polydimethylsiloxane
<b>PR</b>	Photoresist
<b>PVD</b>	Physical Vapor Deposition
<b>RF</b>	Radio Frequency
<b>RIE</b>	Reactive Ion Etch
<b>SE</b>	Secondary Electrons
<b>SEM</b>	Scanning Electron Microscope/Microscopy
<b>UV</b>	Ultra Violet

## Table of Contents

Abstract .....	1
Sammanfattning på svenska .....	2
Acknowledgements .....	3
Abbreviations .....	4
1. Objectives .....	6
2. Background to the field .....	7
3. Fabrication and characterization tools.....	9
3.1 Nanowire and III-V material growth.....	9
3.2 Patterning techniques .....	9
3.3 Deposition of thin films .....	10
3.4 Etching techniques .....	12
3.5 Soft Lithography .....	13
3.6 Scanning Electron Microscopy (SEM) .....	14
3.7 Profilometry.....	14
3.8 Fluorescence microscopy .....	14
3.9 COMSOL modeling.....	15
4 Device fabrication and testing.....	16
4.1 Overview of the fluidic device .....	16
4.2 Fabrication Method.....	17
4.3 Fluidic tests.....	20
5 Results .....	22
5.1 Fluidic device .....	22
5.2 Fluidic tests.....	28
5.3 COMSOL.....	29
6 Discussion .....	30
7 Conclusion .....	31
8 Summary.....	31
9 References.....	32
10 Article.....	34

## 1. Objectives

The aim of this project was to fabricate a device with hollow nanowires connected to a microfluidic system, with the application of injecting molecules into cells. The nanowires, when brought in contact with or penetrating cells, will act as nanoinjection needles through which the molecules to be injected can be transported. The microfluidic channels should be integrated with an external fluidic system to perform controlled and sequential injection with pressure driven flow.

The motivation for developing this device is the ability to transfer substances across biological membranes without adversely disrupting the cell membrane or relying on diffusion which both limits the type and at what rate the substance can be injected and switched. Persson et al. [1] suggested that such a device could be the next step after creating their hollow nanowires on a subsurface channel. The first part of the project aimed towards creating the channels starting from a III-V substrate (semiconductor material created by combining elements from group III and V in the periodic table) and then it continued by investigating the possibility to integrate nanowires in the process. A schematic drawing of how the final device should look like and its functionality can be seen in Figure 1 and the system where the channels on the chip are connected to pumps via microchannels in PDMS is shown in Figure 2. Note that none of the illustrations in this report are to scale.

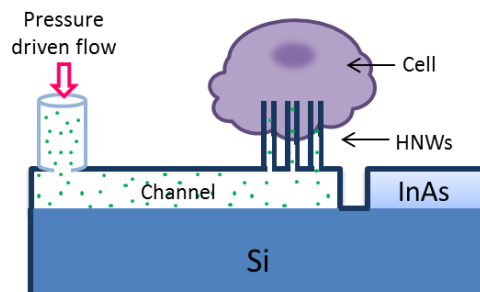


Figure 1. A schematic drawing of the final device. A subsurface channel that can be integrated with both hollow nanowires and attached to an external fluidic system to be able to inject molecules into cells with pressure driven flow.

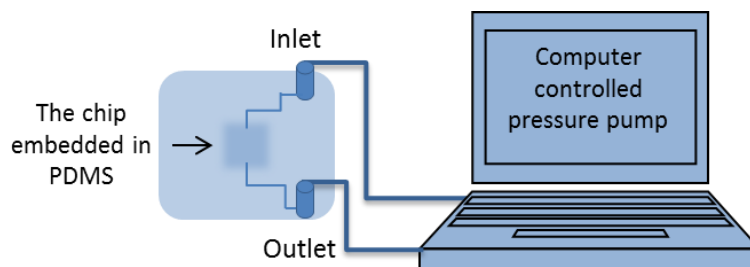


Figure 2. The nanoinjection needle chip is connected to the external pressure pumps via microchannels in PDMS and the HNWs are positioned over the channels on the chip, between the outlet and inlet.

The project was carried out within the biophysics group at the division of Solid State Physics, Lund University, and in cooperation with the company QuNano AB.

## 2. Background to the field

Injecting molecules such as DNA sequences, proteins and drug substances into living cells in vitro is extensively used in biology and life science research today and there are various injection methods which can be both specific and unspecific towards certain cells. Cell injection experiments can be used to study cell functions such as protein regulation, modifying cell gene expression and investigating drug toxicity which is an important step in the development of new medicines.

Some methods used for transporting genetic material into cells are to load carriers with the molecules since they could be too unstable to deliver by themselves. For instance, viral vectors, liposomes and particle bombardment are used for this purpose. Viral vectors are modified viruses which have become highly efficient in transferring genetic material across cell membranes and this method can be used when there is a need to inject molecules into many cells at once [2]. Non-viral vectors such as liposomes are less efficient in the transfer of DNA into the nucleus of the cells; however the technique can be improved by coating them with viral molecules or proteins to increase the uptake [2]. Particle bombardment is used to mechanically force small particles loaded with genes across the membrane by accelerating them to high velocities. This can e.g. be achieved by using a system with compressed gas that generates a shockwave to send the particles towards the cells and because this is mostly a physical process it can be performed on many different cell types and even to cross the cellulose of plant cells [3] [4].

Transfection of the cell membrane can also be achieved in vitro with some permeabilization method such as electroporation or by using calcium phosphate [5]. When exposing the cells to calcium phosphate, pore formation is induced in the cell membrane through which molecules can diffuse into the cytosol of the cell and thus the material to be injected can be inserted just by being kept in the extracellular environment. Electroporation is a more common technique where the permeability of the cell membrane is increased with electrical pulses that cause a dielectric breakdown of the membrane. This breakdown also creates holes in the cell membrane which can function as inlets for molecules and this technique can also be used in combination with any of the carrier-mediated delivery methods [5] [6].

The methods described above are often used when there is a need to inject substances into many cells at once, but they suffer the disadvantages that it is hard to control the amount of material injected in each cell, it puts some restrictions on what type of molecule that can be injected and what type of cell that can receive the substances [3].

An alternative method of injecting molecules into single cells is with microneedle injection. This is carried out with greater control and precision of the injected fluids [7], but since the pipettes are in the same size range as the cells there is a risk of cells rupturing during injection. Therefore, several research groups are now exploring the potential use of injection needles with dimensions at the nanoscale in cellular research since they, due to their small size, might be more appropriate for this purpose. E.g. McKnight et al. [8] have delivered plasmid DNA into cells by attaching it onto carbon nanofibers which allowed cultured cells on top of the fibers to express the gene supplied. The drawback of this technique is that multiple injections are not possible and there are limits to what



type of molecules that can be attached to the fibers. Sköld et al. [9] was one of the first to create injection needles of hollow nanotubes on a thin membrane by using nanowires as templates and they demonstrated their functionality by pulling DNA strands through the wires with electrophoresis, as illustrated in the left drawing in Figure 3. VanDersarl et al. [10] had a similar approach, but created their “nanostraws” by etching down alumina coated nanopores and through a channel underneath, molecules could diffuse through the straws into the cells. In this way they successfully injected green fluorescent protein (GFP) into cells that had been pierced by the needles as exemplified in Figure 3. Peer et al. [11] also showed that they could carry out repeated injection of molecules into cells through nanoneedels without any long-term effect on the wellbeing of the cell, which is an important aspect, and without transfecting nearby cells that were not in contact with the needles. The molecules could diffuse from a reservoir on the back of the chip and the fluid could easily be switched to inject other substances into the cells. Even though these last two approaches opens up for the possibility of multiple injections, they are still slow processes that completely relies on diffusion through the tubes. The methods described above are thus restricted either by the slow process of diffusion or limited to single injections only and fast and serial injections of molecules into cells still remains a problem.

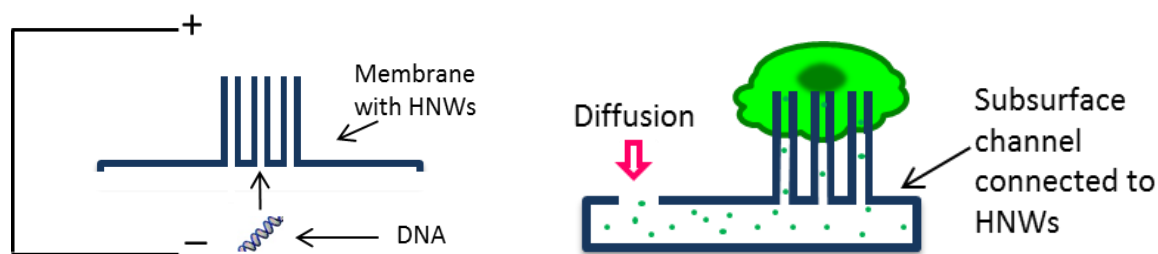


**Figure 3. Left drawing: The principle of the device by Sköld et al. where DNA is pulled through HNW with electrophoresis. Right drawing: GFP diffusing into cells through nanostraws as made by VanDersarl et al.**

Our solution to the above problems is to integrate HNWs to a channel network in a microfluidic device which in turn can be connected to a macroscopic fluidic system, such as pressure pumps. Microfluidic devices are becoming more common analytical tools in biology, chemistry as well as physics and they are used in a wide variety of applications such as separating molecules and fluids, and to analyze cells and proteins [12]. Integrating injection needles with dimensions at the nanoscale with a microfluidic system would enable new applications in cell injection technology such as fast and easy switching of fluids/molecules and repeated injection with increased cell survival compared to micropipettes.

### 3. Fabrication and characterization tools

*In this chapter there will be a short description of the process techniques used to fabricate the device. Note that many of the techniques are used several times throughout the process. In chapter 5 the details of the process scheme can be found.*

#### 3.1 Nanowire and III-V material growth

Compound semiconductor films and nanowires, such as III-V material, can be grown with metal organic vapor phase epitaxy (MOVPE) [13] [14] where at least one of the precursors is in the form of a metalorganic compound which have the benefit of being volatile at low temperatures [15]. The growth generally takes place in a quartz tube kept at atmospheric pressure and the chemical reaction is a function of the gas partial pressure, composition and the temperature in the chamber [14]. In the case of NW growth the reaction is catalyzed with metal particles, often gold, that can be deposited randomly with aerosols or at specific sites after electron beam lithography (EBL, see 3.4) patterning [13]. The growth is then initiated under the particle and leads to vertical pillars with dimensions controlled by the growth time (length) and the gold particle size (diameter) [13].

#### 3.2 Patterning techniques

Electron beam lithography (EBL) and ultra violet lithography (UVL) are two techniques used to pattern polymers (resists) in nano- and microfabrication. While one can resolve smaller structures with EBL, UVL has the advantage of having larger throughput and being cheaper.

##### 3.2.1 Ultra Violet Lithography

Ultra violet wavelengths can be used to create patterns in radiation sensitive polymers, called photoresists, in a lithography system. By exposing the sample through a mask with patterns which are not transparent to UV light, e.g. chromium, the pattern on the mask can be transferred to the resist which then can be used as mask in subsequent process steps. UV lithography is an extensively used technique in nano/micro fabrication and the resolution can be up to 2-5  $\mu\text{m}$  when exposed with a small gap between sample and mask or up to 1  $\mu\text{m}$  in contact mode. [15]

Photo resists are polymers that undergo a structural change when exposed to light. A negative resist becomes insoluble in a developing fluid after exposure, because the polymer chains get cross-linked from the radiation and thus have higher molecular weight. Since the exposed regions are the transparent structures on the mask, the pattern on the sample will be the reverse of the pattern on the mask. When a positive resist is exposed, the polymer chains break and can be dissolved in the developing fluid which means that the pattern transferred will be an exact copy of the pattern on the mask. Photoresists are usually deposited on samples by means of spin coating in which a uniform layer is obtained by pouring a few ml of liquid resist on the sample while rotating it at high speed [15].

##### AZ nLOF 2070 - Negative photoresist

One example of a negative photoresist is nLOF and it is designed to obtain a thickness of around 7  $\mu\text{m}$  when spin coated on samples, but depending on the purpose it can be diluted to attain thinner layers. Smaller structures can be resolved with thinner resist, but when used as etch mask for longer

etch times a thicker resist might be desirable. The resist is i-line sensitive (365 nm) which means it can be used in UV lithography where the exposed resist becomes cross-linked when post-exposure baked and it is suitable for lift-off processes as well as in etches where thermal stability is needed.

### Shipley 1800 - Positive photoresists

Shipley 1800 series are positive resists that are common in microfabrication. The S1818 resist is designed to obtain a thickness of around 2-2,5  $\mu\text{m}$  when spin coated on samples with a speed of 3000 rpm. It is sensitive to wavelengths between 350-450 nm and optimized for the g-line (436 nm). The resist can be used as etch masks and the stability can be increased by post-develop baking the samples.

### 3.2.2 Electron Beam Lithography

Electron beam lithography is a technique in which accelerated electrons are used to directly pattern substrates in nanofabrication without the use of a mask [15]. The electron beam is scanned across the sample on an electron sensitive resist and moved with computer control. Patterns in the submicron range [15] can be resolved and the resist can be used as mask in future fabrication steps. EBL can be used to define sites where NW growth should be initiated, as illustrated in Figure 4, and with these EBL defined growth sites the NWs can be positioned in well-defined patterns to match structures of future devices [16].

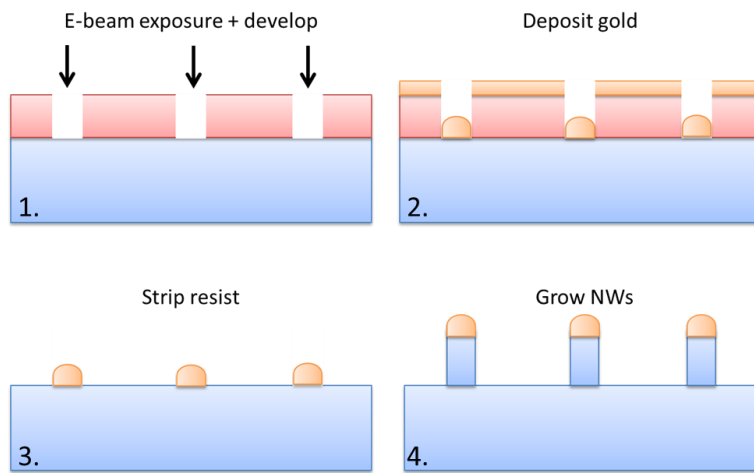


Figure 4. The process to use EBL to define where NW growth should be initiated.

Electron resists are polymers that function in a similar way to photoresists, but the structural change is induced by the polymer-electron interaction instead of absorbing the energy from the light. The exposed regions of a negative electron resist becomes less soluble after exposure to the electron beam whereas it becomes more soluble for a positive electron resist. [15]

### 3.3 Deposition of thin films

Atomic layer deposition and sputtering are two techniques to deposit thin films. An ALD film is extremely conformal and built with a greater accuracy than sputtered films. The sputtered films on the other hand can be deposited at a faster rate when there are less requirements of film quality.

### 3.3.1 Atomic Layer Deposition

Atomic layer deposition is a chemical vapor deposition (CVD) method to create thin films of metals and oxides with extreme conformity and quality. As the name implies, the conformity is achieved by adding one atom layer at a time in cycles until the desired film thickness is reached. The mechanism behind the technique is that precursors of the film material are sequentially pulsed into the process chamber at a temperature so that the reactions are selfterminating [17]. To deposit aluminum oxide ( $\text{Al}_2\text{O}_3$ ), the precursors used are trimethylaluminum (TMAI) and  $\text{H}_2\text{O}$  and they are separated by an evacuation of the chamber to remove unbound precursor species as shown in Figure 5.

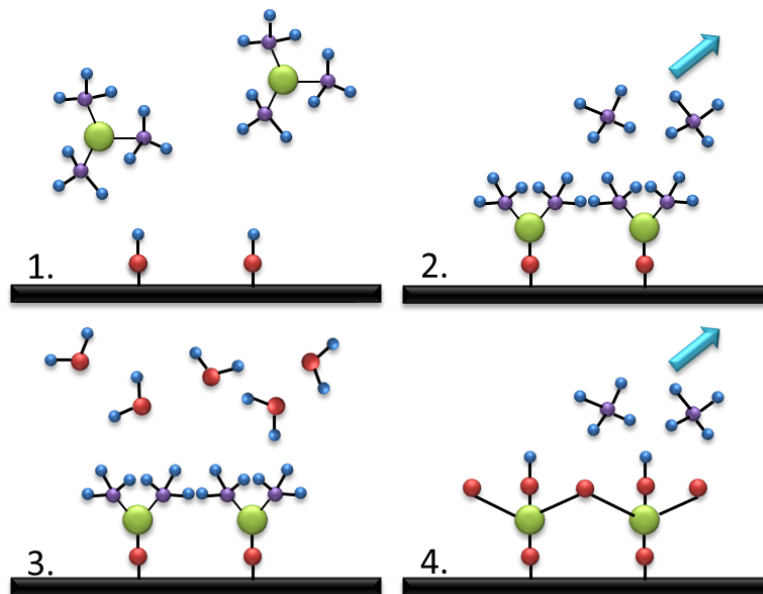
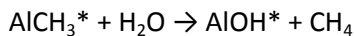
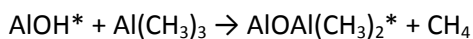
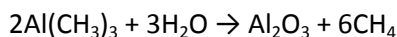


Figure 5. One cycle in the ALD process to generate  $\text{Al}_2\text{O}_3$ . 1: TMAI is pulsed into the chamber and approaching a hydroxyl terminated surface. 2: The aluminum atom binds to the oxygen atom and methane is removed as rest product. 3:  $\text{H}_2\text{O}$  is pulsed into the chamber. 4: The oxygen atom binds to the aluminum atom and methane is removed as rest product. One atomic controlled layer of  $\text{Al}_2\text{O}_3$  is created.

The self-limiting reactions in each cycle are [18]:



Where the asterisk indicate which species are at the surface and thus where the next molecule binds. This gives the total reaction for generating  $\text{Al}_2\text{O}_3$



The deposition is self-limiting since the number of functional groups on the surface can be controlled and will only react until these sites are filled.

### 3.3.2 Sputter Deposition

Sputtering is a physical vapor deposition (PVD) technique to deposit thin films, which is faster than ALD, but the obtained film does not have the same quality. The deposition takes place in a chamber at low pressure and the material to be deposited, called target material, is situated on a negatively biased electrode opposite the sample as schematically seen in Figure 6. A process gas, typically an inert gas such as Ar, is introduced into the chamber and when an electric field is applied free electrons will be accelerated and ionize the process gas, generating a plasma of positive Ar ions. These ions will accelerate towards the negative target electrode and the energy transfer will remove material from the cathode upon impact, called sputtering removal. The sputtered particles will deposit on the sample and everywhere else in the chamber and by rotating the sample holder an even film of the target material can be obtained on the surface. Magnetron sputtering is a further improvement of this technique where the plasma is contained close to the target material by the aid of a magnetic field [19]. This will result in less sputtering removal from the sample and enhanced efficiency of sputtering from the target since the plasma density is increased. The power supply can be either of direct current (DC) or radio frequency (RF) type and the latter makes it possible to sputter insulating materials [20].

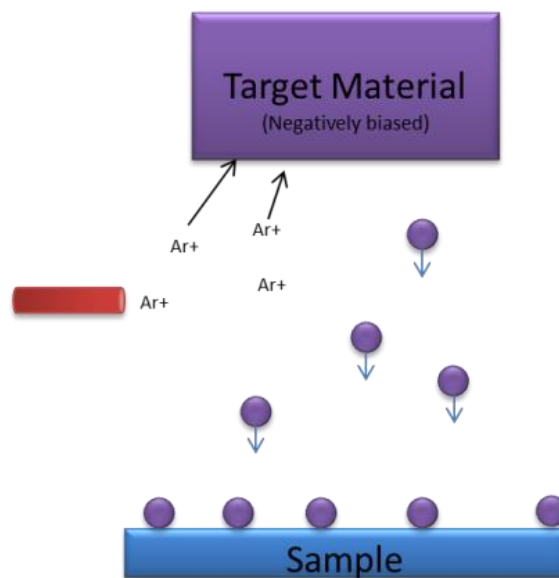


Figure 6. The sputter deposition process.

### 3.4 Etching techniques

Etching is removal of material, often from samples in semiconductor device fabrication. It is either carried out with acids (wet etch) or by creating a plasma with reactive species (dry etch) which are allowed to react with the sample. The used etchant should have a high selectivity against other materials, meaning that a certain material etches faster than other. It is often desired that the removal of material is carried out in a directional manner, referred to as anisotropic etch. However, in some cases isotropic etch is preferred in which all directions etches equally fast.

### 3.4.1 Inductively Coupled Plasma Reactive Ion Etch (ICP-RIE)

Reactive ion etch (RIE) is a chemical and physical dry etch process technique in where etchant species are generated in plasma and reacts with the sample surface material [15]. In the inductively coupled plasma (ICP) configuration, high energetic plasma is created in a vacuum chamber by applying a radio frequency (RF) magnetic field to a coil surrounding the process gases. The substrate holder is powered by a separate source and biased negatively causing the positive ions in the plasma to be accelerated towards the sample. The chemical process can be selective and this selectivity is obtained by the use of different process gases. The physical process comes from energetic positive ions that impinge everywhere on the surface (sputtering removal) and this process is less selective but often create etch profiles that are more anisotropic than chemical etching [15].

The inductive coupling is used to increase the plasma density and the ICP-etchers often operate at lower pressures [15]. The higher density of the plasma will lead to increased etch rate of the material since a faster reaction will take place. The parameters affecting the etch rate of materials are the process gases used, the gas flows, the pressure in the chamber, the RF power, the ICP power and the material of the substrate holder (lower electrode).

### 3.4.2 Wet Chemical Etch

Wet etching is carried out by immersing a sample in an etchant fluid and in microprocessing, selective etching of certain materials is important knowledge not to destroy structures of materials that should remain. The profiles created are often isotropic, although some etchants prefer to etch specific orientations in crystalline materials, creating more anisotropic etch profiles [15]. Wet etch can more easily reach into narrow structures, such as channels, than dry etch which mostly attacks the exposed surface.

## 3.5 Soft Lithography

Soft lithography is a molding technique to create structures with dimensions at the nano- and microscale in elastomeric material, such as polydimethylsiloxane (PDMS). A template of the reverse of the structure is used as a stamp that mechanically deforms the material to be patterned. The template can be created with several techniques, e.g. with photolithography, and it can be used several times, which is cost effective and easy fabrication. Furthermore, the structures can be created on non-planar surfaces and in a wide variety of materials, not only on resists which is the case for photolithography. [21]

Plasma bonding can be used to covalently bond surfaces together. The pieces that should be bonded together are exposed to oxygen plasma which introduces hydroxyl groups on the surfaces and when brought in contact, they form an irreversible bond. Plasma bonding is a commonly used technique to bond PDMS to surfaces for microfluidic applications. [22]

### 3.6 Scanning Electron Microscopy (SEM)

One extensively used characterization technique in microfabrication is scanning electron microscopy (SEM) in which electrons that are accelerated by a high voltage are used to create an image of the sample. The electron source can be either a thermionic emitter or a field emitter and the electrons are focused to a beam with electromagnetic lenses and scanned across the surface of the sample. When the electrons impinge on the sample they give rise to many signals such as secondary electrons (SE), backscattered electrons (BSE), auger electrons (AE) and x-rays. A wide variety of information can be obtained from the various signals such as images of the surface, local crystal structure and elemental analysis of the sample. When creating images of surfaces, SE are one of the most common signals to detect. SE arise from inelastic scattering of the beam electrons in the sample and the mean free path of these low energy electrons are short. Thus the SE that are detected here are created at the surface, which means that images of the topography of the surface can be obtained. [23]

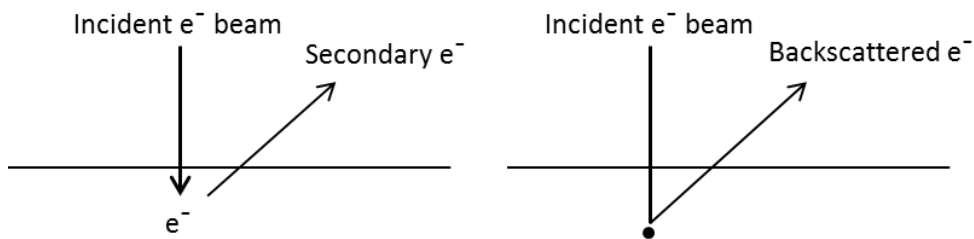


Figure 7. Different signals in SEM. The SEs are electrons that are knocked out from atoms in the sample whereas the BSEs are the incident beam electrons that have scattered against atoms in the sample.

### 3.7 Profilometry

A profilometer is an instrument that can be used to measure surface profiles of samples at the nanometer scale. A thin tip is moved across the sample with a set force and the vertical displacement of the tip can be used to create a 2D profile of the surface. Measuring depths on samples after etch procedures is an important tool in determining etching rates when developing new processes [24].

### 3.8 Fluorescence microscopy

Fluorescence microscopy refers to the method of imaging fluorescent molecules in optical microscopes (OM), which is common in biology. A fluorescent dye, a fluorophore, is a molecule that can be excited to a higher energy state by absorbing photons. When the molecule is de-excited it loses some energy by relaxation and the rest of the energy is emitted as a photon with longer wavelength than the absorbed light. This light can be studied clearly in an OM by using a filter to remove all other wavelengths. Even single fluorescing molecules can be seen, making this technique extremely sensitive [25]. By injecting a fluorescent dye mixed with a fluid into micro channels it is possible to see the fluid moving in these small structures much clearer than if trying to study the fluid only and due to its sensitivity, it is also easier to detect a small potential leakage in the channels.

### 3.9 COMSOL modeling

COMSOL Multiphysics is a software created to model and run simulations of physics related problems. Since the design of the device only was a test-structure, one part of the project was also to aid in the development of a new improved design. Modeling of the flow in the channels was performed in COMSOL to obtain an understanding of what the new design should look like to get a homogenous mixture in the small chamber over which the nanowires should be positioned. Modeling was carried out both on the test structures already created by QuNano and then an improved design was modeled.



## 4 Device fabrication and testing

In this chapter the fabrication of the device will be explained and a simplified process scheme is illustrated in Figure 8. The method used to carry out the fluidic tests will be explained towards the end of the chapter.

### 4.1 Overview of the fluidic device

The device has been fabricated from a test design first proposed by QuNano AB. The channels are all 5  $\mu\text{m}$  wide and with varying lengths and shapes. The fabrication have started from planar InAs substrates and thin oxide channels are created which are surrounded by support structures of oxide covered InAs.

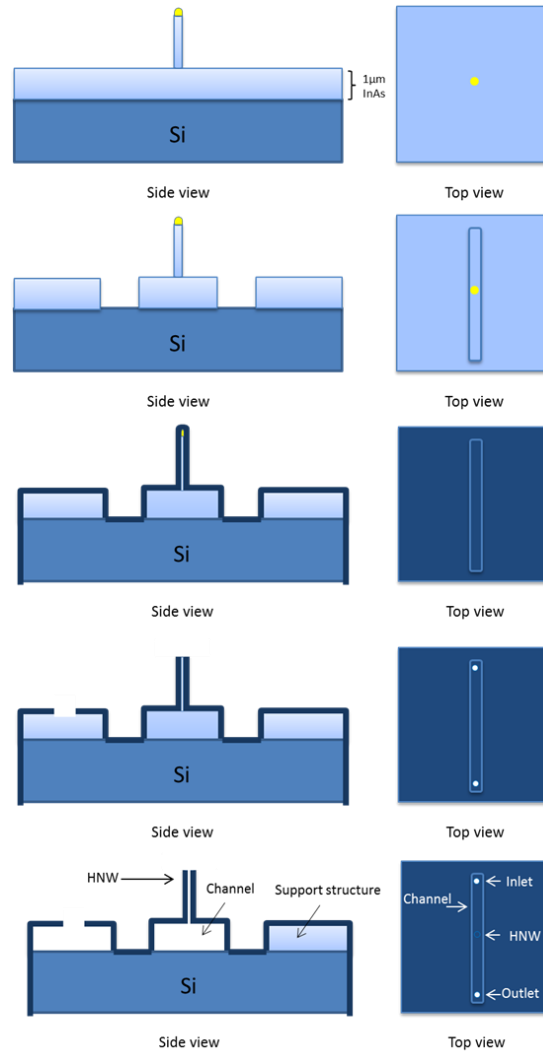


Figure 8. A simplified process scheme 1. NWs are grown on a thick InAs buffer on a silicon substrate. 2. The InAs is etched down with RIE on the sides of the wires in long channel-like structures with an etch mask defined with UV-lithography. 3. The whole sample and the wires are covered in  $\text{Al}_2\text{O}_3$  using ALD. 4. Openings in each end of the channels are created and the tips of the NWs are removed. 5. The InAs in the channels are removed with wet etch, leaving hollow nanowires connected to a channel of  $\text{Al}_2\text{O}_3$  and the remaining InAs will act as mechanical support for the channels.

## 4.2 Fabrication Method

While fabricating this device there are some things that need to be kept in mind. First, the materials in the final device need to be biocompatible since it is developed for experiments on living cells. Second, the material of the fluidic system needs to be strong and intact because it has to be able to withstand the pressure of fluids being pushed through the channels without breaking or leaking. The fabrication starts with the creation of microchannels from planar InAs buffer substrates by using varying top down and bottom up process techniques. It follows with an investigation of the possibility to integrate semiconductor nanowires as templates for the needles; therefore the nanowires are considered all the way.

### 4.2.1 InAs growth and ALD deposition

An InAs buffer was epitaxially grown with MOVPE, in equipment from Aixtron and the precursors used were TMIn and AsH<sub>3</sub>. When NWs are integrated in the process they will be positioned with EBL defined patterns on top of the buffer, in the area where the channels are supposed to be. After the growth, the sample was covered with 200 cycles each of ZnO and Al<sub>2</sub>O<sub>3</sub> with ALD. The layer of Al<sub>2</sub>O<sub>3</sub> will act as a support layer for the NWs, when they are in the process, during following process steps since the wires will be really easily broken due to their small diameters. The ZnO was closest to the InAs in order to shorten the time in which the channels are etched through, as will be described in section 5.1.4.

### 4.2.2 Channel Outline

To create channels in the buffer, the InAs need to be etched down all the way to the Si substrate in channel like patterns, as was illustrated in Figure 8. The etched down area will outline walls of the channel and the remaining InAs between the walls will be the channel in the end. The InAs etch should be anisotropic to obtain straight walls, and therefore dry etch was a preferred method. A chemistry of CH<sub>4</sub>/Ar/H<sub>2</sub> with a low pressure (5mTorr) in ICP RIE has shown to etch InAs with reasonable etch rate and generate smooth and vertical etch edges which is why an etch process with similar parameters was developed [26]. Due to the relatively thick InAs buffer that needed to be etched down completely, several etch masks were proposed for this purpose.

A hard mask was deposited on the two ALD layers, which means that it was three layers that needed to be etched before the InAs buffer could be reached. UV-lithography was used to pattern channels on top of the layers and then the hard mask and the Al<sub>2</sub>O<sub>3</sub> layer were etched with this PR as mask in RIE and ICP RIE respectively. After this step, the PR could be stripped, either in a solvent or removed in O<sub>2</sub> plasma depending on the type of resist used. Both nLOF and hard baked S1818 was being tested in this step. The ZnO and the InAs layers could now be etched with similar parameters in ICP RIE and the process flow to define the channels is shown in Figure 9.

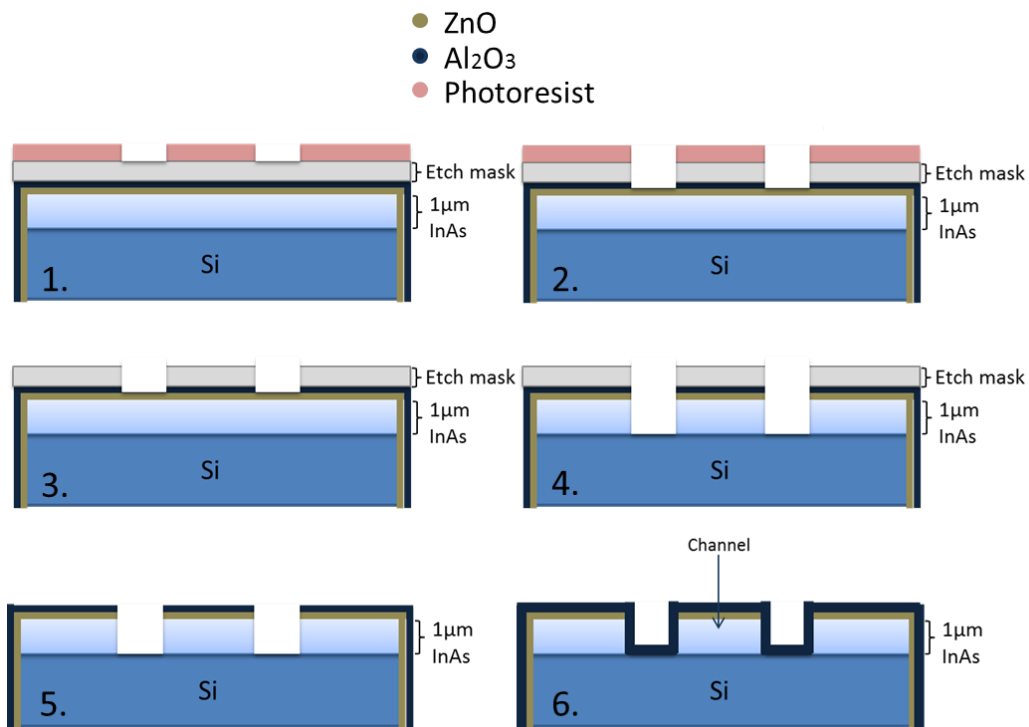


**Figure 9. Cross section of the sample demonstrating the fabrication steps used to create a wall around an InAs channel.**  
**1. Pattern the hard mask with PR. 2. Etch the hard mask and the support layer of  $\text{Al}_2\text{O}_3$  with PR as mask. 3. Strip PR. 4. Etch ZnO fast-etch layer and InAs with the hard mask. 5. Remove the hard mask. 6. Deposit 1000 Å  $\text{Al}_2\text{O}_3$  with ALD as a wall for the channel.**

It is extremely important that all InAs was removed in the etched down structures; otherwise there is a large risk that the wet etchant used in later process steps could spread in InAs residues and outside the channel area, causing the structures to collapse. The complete removal of InAs was easily confirmed by studying the samples in SEM prior to wall deposition.

Once the walls were defined, the mask could be removed and the final step was to create the actual channel wall which is a layer of 1000 cycles  $\text{Al}_2\text{O}_3$  deposited with ALD. The  $\text{Al}_2\text{O}_3$  forms a continuous film over the InAs buffer that is left, as can be seen in the last illustration in Figure 9.

#### 4.2.3 Creation of Channel Inlets/Outlets

Since the whole sample was completely covered in  $\text{Al}_2\text{O}_3$  from the ALD there was a need to open up holes in the film in each end of the newly outlined channels, in order for the etchant to reach the buffer underneath. These holes would also work as the inlet and outlet for the fluidics. The openings were quite narrow and dry etch was used for this step as well to obtain well defined holes.

$\text{Al}_2\text{O}_3$  can be etched in ICP RIE with  $\text{CF}_4/\text{H}_2$  chemistry, as was also used when the support layer in the channel walls was etched.  $\text{Al}_2\text{O}_3$  is in general quite difficult to dry etch, since it is a hard material, but with high ICP power an etch rate of  $\sim 150 \text{ Å/min}$  could be obtained. A UV- lithography step was used to define the openings and the PR was used as a mask during the etch. A thick photoresist was

desirable since this etch has low selectivity against photoresist. If the PR would be etched fast enough, there is a risk that the underlying  $\text{Al}_2\text{O}_3$  would start to be removed which would destroy the channel wall. On the other hand, the lithography for this step demanded resolving circular holes with diameters of  $3\text{ }\mu\text{m}$ , since they needed to be aligned and fit in channels with a width of  $5\text{ }\mu\text{m}$ . This is in the limit of what can be achieved with soft contact UV lithography and because of this it was difficult to use thick PR, so this really was an optimization problem.

#### 4.2.4 Freestanding Channels

Once openings in the  $\text{Al}_2\text{O}_3$  are formed, the InAs could be removed with wet etch to create hollow channels, which is illustrated in Figure 10. Only the InAs in the channels was supposed to be removed in this step, since the remaining InAs on the sample would act as mechanical support for the channels during the load of a cell. The width of the channels was  $\sim 5\text{ }\mu\text{m}$  whereas the supporting structures could be up to several mm wide (figure 10 is not drawn to scale) and if the InAs would be removed under that large areas of  $\text{Al}_2\text{O}_3$  the whole structure would collapse. Furthermore, if the structures would collapse in the close vicinity of the in- and outlets, tightly sealed fluidic connections would be hard to realize and the fluidic tests would show dyes leaking throughout the sample. Because of this, there was a need to protect all areas of the sample from the etchant except the small in- and outlets for the channels.

A layer of a benzocyclobutene based resin (BCB 3022-46, DOW Company) was spin coated onto the samples and cured in a  $\text{N}_2$  environment to prevent the etchant to reach the InAs through pinholes in the  $\text{Al}_2\text{O}_3$  film on the front. Because of poor adhesion between  $\text{Al}_2\text{O}_3$  and BCB, a layer of  $\text{SiO}_2$  was sputtered on top of the  $\text{Al}_2\text{O}_3$  as an adhesion layer. Both BCB and  $\text{SiO}_2$  could be patterned and etched in  $\text{CF}_4/\text{O}_2$  chemistry in RIE to create openings for the etchant.

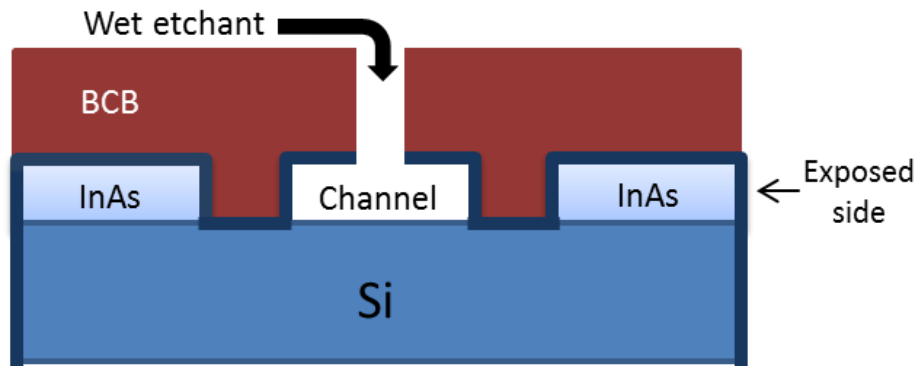


Figure 10. Cross section through the sample. The front side of the sample can be protected from etchant with BCB but the sides are still exposed.

The front side of the sample was covered in BCB, but the edges were still exposed and risking to be reached by the etchant, as shown in Figure 10. Several attempts were made to prevent the InAs to be exposed on sides, such as cover the edges with some polymers (S1818 and PDMS) and also to only place drops of the etchant on the top of the sample so that the edges were never in contact with the acid.

Since the channels are long and narrow, the etch rate in the channels seemed to be limited by diffusion of etchants into the channels and etch products out. Several wet etch techniques were tested in order to optimize this process step. To shorten the etch time, a layer of ZnO was deposited on top of the InAs as a first process step for the device as described in 5.1.1 and shown in Figure 11. ZnO etches extremely fast in HCl, much faster than any method tested to etch InAs, which is why it was chosen for this purpose. By first immersing the sample in HCl the ZnO can be removed which creates a pocket in the top of the channels where the etchant for InAs can reach and thus the etch time for the InAs can be shortened significantly, see Figure 11. The thickness of the ZnO layer will contribute to the width of the inner diameter of the HNWs though, which is why a fairly thin layer still must be used.

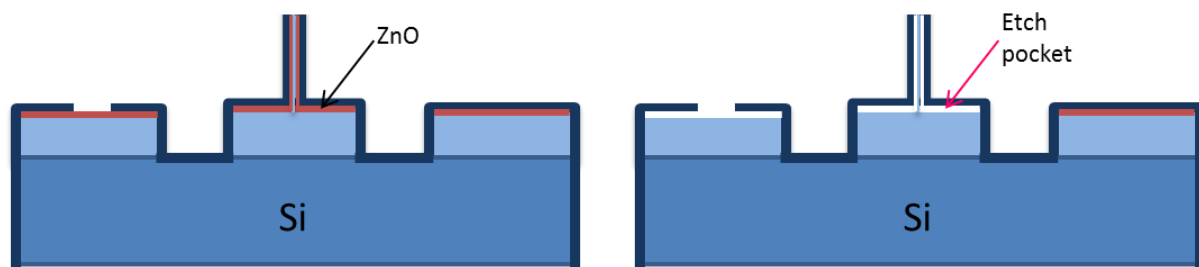


Figure 11. A layer of ZnO in the top of the channels can be etched really fast in HCl, creating a pocket where the etchant for InAs can creep in order to etch through the channel faster.

#### 4.2.5 External fluidic attachment

The final step in the process was to attach a piece of PDMS with microfluidic channels on top of the sample in order to link the hollow channels of  $\text{Al}_2\text{O}_3$  to a pressure pump. PDMS is a material widely used in microfluidic systems due to its flexibility and the way it can be bonded to a variety of substrates. The liquid, uncured PDMS was mixed with a catalyst at a ratio of 1:10 and molded on a SU8-master with soft lithography. The channels on the SU8-master was defined with UV-lithography and they matches the in- and outlets of the channels on the sample.

The PDMS was bonded onto the sample after exposing them both to a 60s  $\text{O}_2$  plasma treatment. The  $\text{O}_2$  plasma also makes the channels hydrophilic which makes it easier to push fluids through them. At the ends of the PDMS channels, holes were opened up and small silicone tubes were glued over the openings. These tubes were used to attach the external fluidic pumps.

### 4.3 Fluidic tests

In order to test the functionality of the device a first step was to see if it was possible to run fluids through the channels to confirm that they had not collapsed. The tubes on the PDMS microchannels were filled with a couple of  $\mu\text{l}$  of ethanol mixed with a fluorescent dye. The tubes were then connected to a pressure pump and pressures,  $p$ , ranging from 0 to 50 mbar were applied. Before

starting, the sample was positioned on an OM equipped with a camera and filters to enable studying the dye in the channels during injection.

The pressure-driven flow (Poiseuille flow) in the channels gives a theoretical velocity,  $v$ , by [12]

$$v \sim \frac{\Delta p w^2}{\eta l} \quad [\text{Equation 1}]$$

Where  $w$  is the radius of a circular channel,  $\eta$  is the viscosity of the fluid and  $l$  is the length of the channel. By using the channel length of 2 mm and approximating the channels to be circular with a radius of 1  $\mu\text{m}$  a theoretical velocity of  $\sim 2$  mm/s is obtained. This was calculated by using the viscosity for ethanol of 1.20 mPas (at  $T=293$  K).

## 5 Results

*This chapter aims to describe the results obtained during the whole project and is divided into the separate parts of the final device, the fluidic tests and the modeling.*

### 5.1 Fluidic device

The final fluidic device with PDMS attached can be seen in Figure 12 where the channels in the PDMS have connected tubes for the pressure pump. Figure 13 is an OM picture of three parallel channels, where the large circular hole defines where the BCB is open and the “halo” around the channels is the only remaining InAs. As seen, the channels are really narrow with small circular holes in one end, which has been the inlet for the etchant and outlet for the etch products throughout the channel. The separate fabrication results are described below.

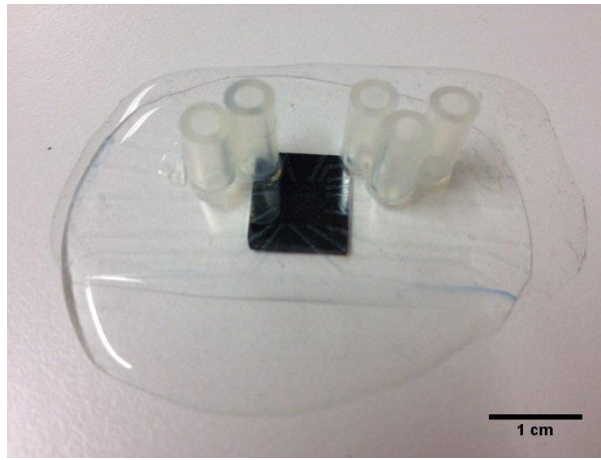


Figure 12. One sample embedded in PDMS with attaches tubes ready for fluidic tests.

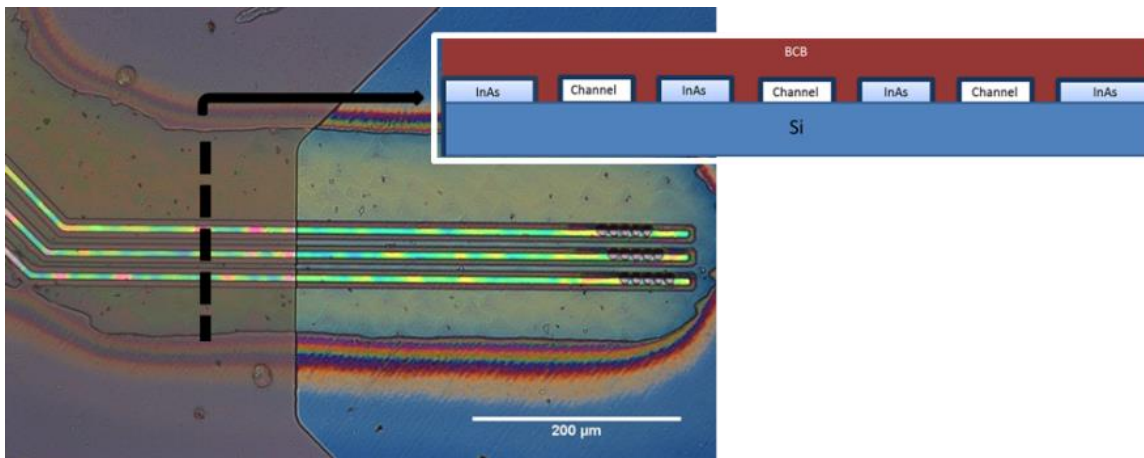


Figure 13. Channels of  $\text{Al}_2\text{O}_3$  embedded in BCB (large opening) and the “halo” around the channels is the supporting InAs. A cross section of the three channels is illustrated in the inset.

### 5.1.1 Etch mask development

In order to dry etch the InAs, several etch masks were proposed and tested. The obtained etch rate in the  $\text{CH}_4/\text{Ar}/\text{H}_2$  chemistry was  $\sim 20$  nm/min which means that the time needed was 50 min in ICP-RIE to etch down the buffer layer ( $1\text{ }\mu\text{m}$ ). The mask needed to be resistant throughout the etch and not degrade since it should protect the channels, and later also the NWs. The qualities of the etch masks tested are summarized in Table 1.

#### ***S1818 (Shipley photo resist)***

Tests with this photoresist did not generate the vertical walls that were a requirement for the process. The results also varied and were quite unreliable on tests where the buffer was only 300 nm thick, so whether the photo resist mask could last for etching thicker buffer was very questionable. Additionally, when InAs is etched with this chemistry, polymer formation occurs. This is a known problem, and the deposits on the sample are hard to get rid of [26]. A hard mask was therefore developed which would serve both as protection of the wires during the etch and since it would be removed after the etch, residues deposited on top could be removed in the same step.

#### ***Silicon dioxide ( $\text{SiO}_2$ )***

The first choice of hard mask material was  $\text{SiO}_2$  which previously had been used in similar etches [27]. Vertical walls could be obtained and since  $\text{SiO}_2$  can be removed with both dry and wet etch, it was also possible to get rid of the polymerized residues. Unfortunately sputtered  $\text{SiO}_2$ , which was the available choice, showed to be quite unpredictable for this long etch time and very sensitive to what types of process gases were used previously in the ICP RIE. The unreliable stability of  $\text{SiO}_2$  made it a less attractive choice as hard mask.

#### ***Wolfram and Chromium***

Wolfram (W) and chromium (Cr) were both tested for their potential use as masks in this etch instead and neither of these metals seemed to be affected much. Some visible changes on the metal surfaces were observed but no measureable etch depth in profilometer. The reason W was chosen was because it is easier to dry etch than Cr and it was tested as hard mask for  $1\text{ }\mu\text{m}$  InAs buffer where it showed excellent performance with reproducible results in the channel wall formation. The result can be seen in Figure 14.

Table 1. All etch masks tested and their qualities while dry etching InAs.

Mask	Vertical walls	Stability in etch	Possible to dry etch
<b>S1818 (resist)</b>	No	-	-
<b><math>\text{SiO}_2</math></b>	Yes	Varying	Yes
<b>Cr</b>	Yes	Yes	Difficult
<b>W</b>	Yes	Yes	Yes



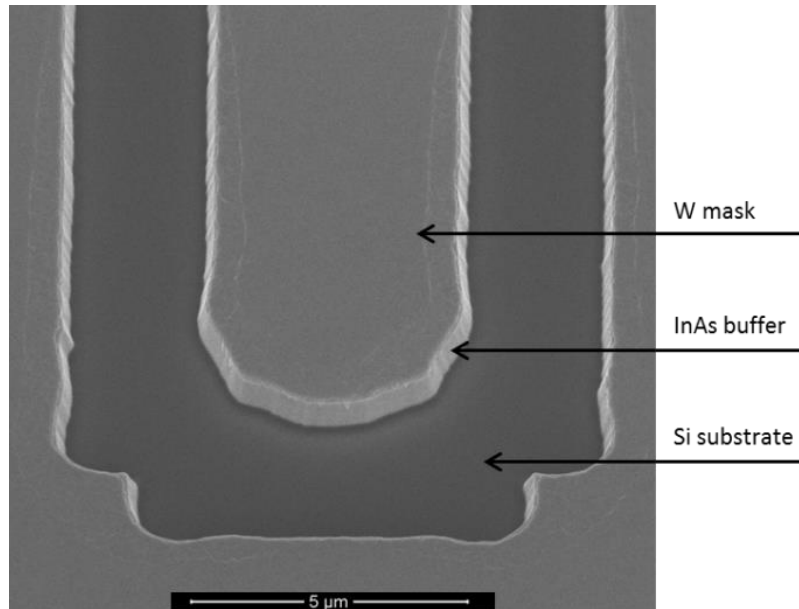


Figure 14. SEM image of the end of a channel seen from 30° tilt. Smooth, vertical edges are obtained in the InAs when etched in ICP-RIE with  $\text{CH}_4/\text{Ar}/\text{H}_2$  chemistry and by using tungsten as etch mask.

### 5.1.2 Defining channel walls

Once the etch mask was developed it was used when defining the channel walls. In Figure 15 one can see two SEM images where the left one has InAs residues in the etched down area. These were found to arise from insufficient etch of the mask material (W) after the lithography patterning and could be corrected with additional 20 s RIE etch of the tungsten mask. In the right image smooth, vertical walls can be seen with most InAs residues removed and less risk for the channels to leak.

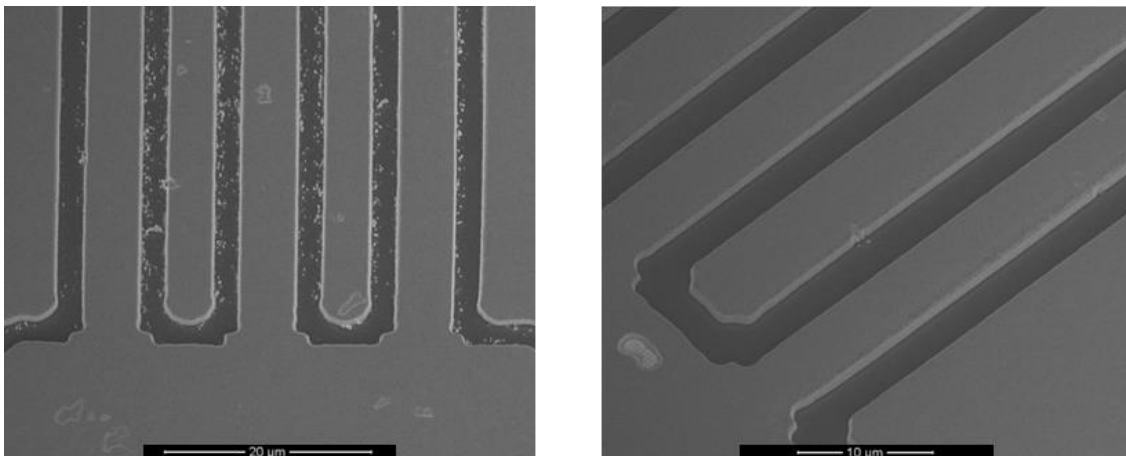


Figure 15. Left: InAs residues in the etched down area due to insufficient W-etch. Right: Longer etch time has decreased the residues significantly.

### 5.1.3 Creation of channel inlets/outlets

Small holes at the channel ends were opened in the  $\text{Al}_2\text{O}_3$  as seen in the SEM image in Figure 16. In this step it was first found that several of the channels had broken off from the substrate during the aggressive etch in ICP RIE as seen in Figure 16. By studying the bottom of the channel through the opened holes it was concluded that the width of the bottom had decreased to less than half the width of the top of the channel. During further tests it was found that while removing the hard mask of W after the InAs dry etch, the exposed Si substrate also was attacked and that it was etched isotropically. Since the isotropical etch reaches underneath the channel it becomes unstable causing it to break and the created profile can be seen in the drawing in Figure 16. A shortening of the hard mask removal etch solved this problem and no channel break offs were observed after this.

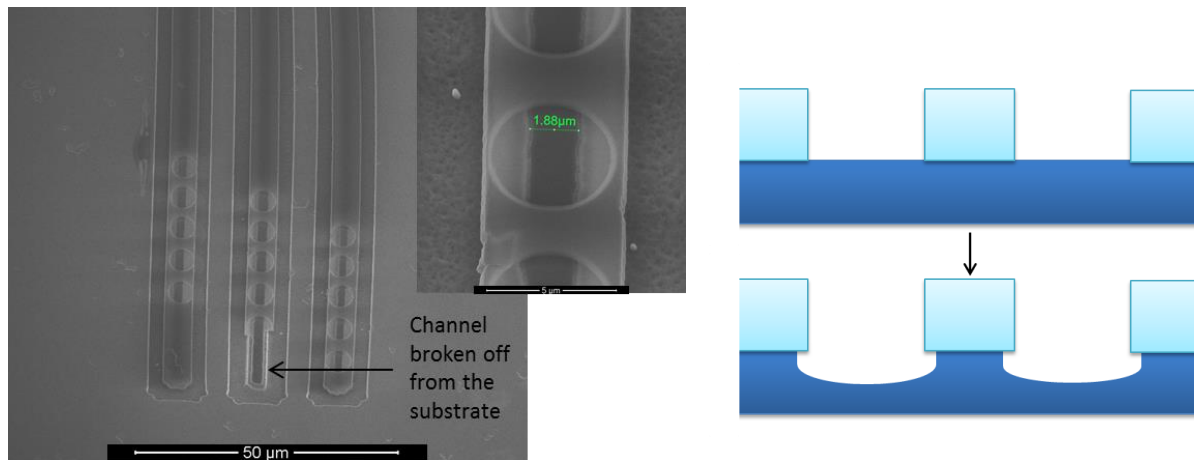


Figure 16. Left: SEM image of the channel openings of three parallel channels. The zoomed in picture shows that the bottom of the channel is less than half of the width of the top of channel. One channel has completely broken off from the surface due to the instability. In the illustration to the right one can see how the desired etch profile have turned to an under etched structure.

### 5.1.4 Creation of hollow channels

Several wet etchants were tested to etch through the channels in the creation of hollow structures. The requirements are that the etchant should not attack either Si or  $\text{Al}_2\text{O}_3$  and the etch rate should also be high, since the structures are long and narrow. The etch rate also decrease further into the channel because of the diffusion of reactants and products in and out.

#### ***HBr/HNO<sub>3</sub>/H<sub>2</sub>O***

A mixture of HBr/HNO<sub>3</sub>/H<sub>2</sub>O was found the etch InAs very fast, but unfortunately this etchant also etches the Si which means that it cannot be used since the channels are standing directly on the Si substrate. During the tests with these acids the etchant spread underneath the channel walls and caused the whole structure to collapse.

#### ***Aqua Regia***

Aqua regia (HCl:HNO<sub>3</sub>, 1:3) also etches InAs fast on open structures, but in long narrow channels the etch rate is extremely slow. Even though the channels are open on both sides, ~24h in aqua regia would be needed to etch the shortest channel on the test design which had a length of less than 2 mm.

### ***Citric Acid:Hydrogen Peroxide***

Citric acid mixed with hydrogen peroxide was also tested to etch through the channels, and it is a less harmful etchant than the previously described acids, which needs to be considered for these long etch times. Unfortunately, the etch rate was decreased substantially which may either depend on the weaker reaction between the etchant and InAs or that the citric acid molecule is larger than the other molecules and therefore more affected by the diffusion barrier.

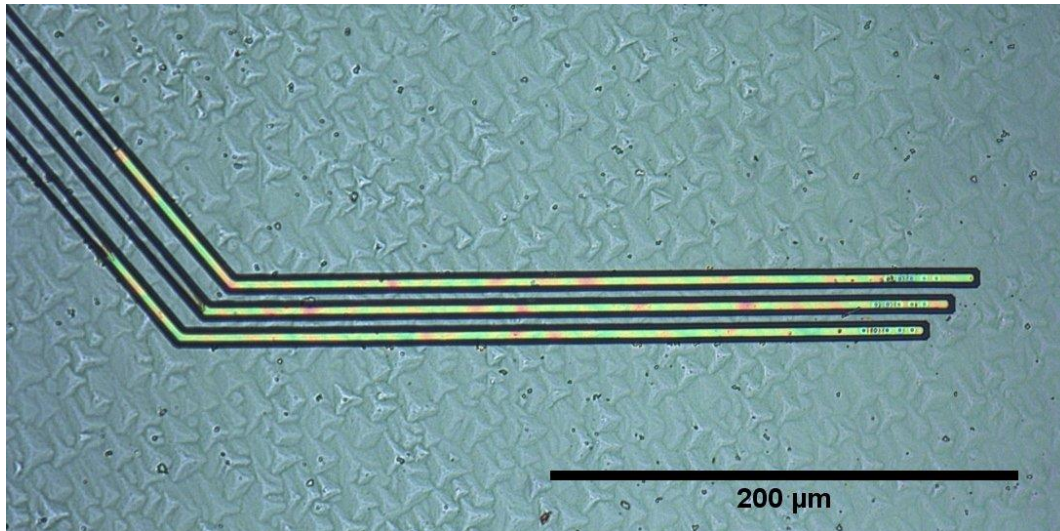


Figure 17. Aqua regia spreading in microchannels of  $\text{Al}_2\text{O}_3$ .

### ***With ZnO in the channels***

Since none of the above methods gave desired results the method with ZnO in the top layer of the channels were developed. By first immersing the sample in HCl (37%) diluted with equal part of  $\text{H}_2\text{O}$ , the ZnO could be etched first and then the InAs could be removed in aqua regia. With this process the etch time could be reduced to half compared to if the InAs would be etched with aqua regia only. A further shortening of etch time might be possible by completely drying out the channel after all ZnO was removed which would allow the aqua regia to move faster in the pocket with capillary forces, but not enough tests were carried out to conclude this.

### **5.1.5 Protect remaining InAs support structures from etchants**

It was at an early stage found that the  $\text{Al}_2\text{O}_3$  layer is not enough to protect the InAs in the remaining structures from being etched. Pinholes created in the film gives an access to the InAs and the etchant spreads much faster there than in the narrow channels, an example can be seen in Figure 18. The BCB layer served as an excellent protective film on the front of the sample, but the sides were still exposed to the acids. All attempts (cover the edges with hardbaked resist, embed the sample in

PDMS, etch with only small droplets) to protect the edges failed, since the etch time needed was at least 12h and none of these protections could keep the acid out that long.

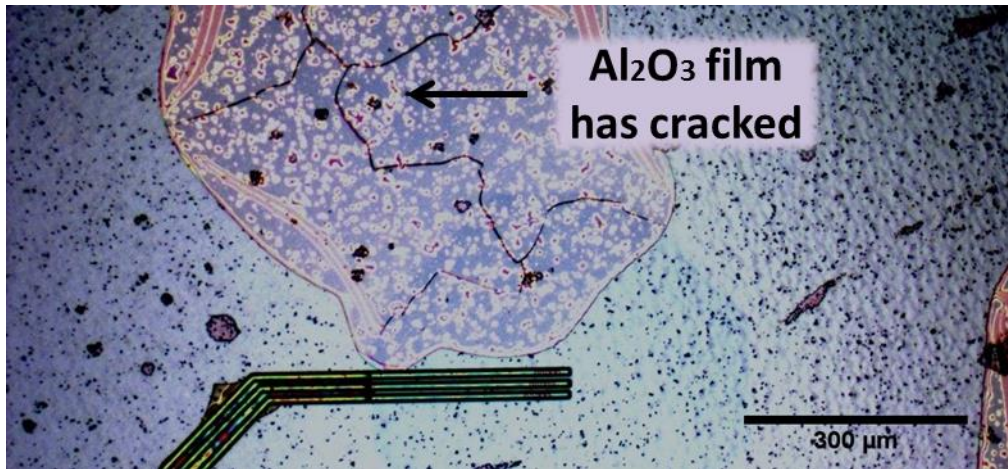


Figure 18. The etchant has reached the InAs through a pin hole in the Al<sub>2</sub>O<sub>3</sub> which has caused the film to crack and the etchant is spreading under the film towards the channel.

Since cured BCB resin resembles SiO<sub>2</sub> it could be used to stabilize the channels by itself which is why the next design would have almost all InAs throughout the sample removed and the hollow channels embedded in BCB. This solved the problems with collapsing structures and the channels could be etched through without problems.

#### 5.1.6 External fluidic attachment

Different ways to bond PDMS to the sample have shown different results in terms of flow in the micro channels. Both bonding of PDMS with O<sub>2</sub> plasma and half cured PDMS have been tested and the alignment of the channels to each other was achieved either by aligning through a microscope or by sliding the surfaces in place with ethanol in between which delays the irreversible bonding until the ethanol has evaporated.

Bonding without any O<sub>2</sub> plasma showed some problems when a mixture of water was first injected, indicating that the channels may have become hydrophobic. When the O<sub>2</sub> plasma bonding technique was used it was easier to push fluid through the channels, but still ethanol was easier than water due to its lower surface tension. Furthermore, when one device was tested twice with one week separation, the flow rate in the channels for the ethanol had decreased significantly which indicates that the OH-groups introduced with the O<sub>2</sub> plasma diffuse into the PDMS and the channels turn from hydrophilic to hydrophobic again.

#### 5.1.7 Basic tests with nanowires

Some basic tests were carried out on samples with nanowires in order to find out what type of resist to use in the different process steps to ensure that the wires do not break. It was found that the wolfram layer serves well as an etch mask also when there are nanowires in the process, which probably would not have been the case with only photoresist as a mask.



## 5.2 Fluidic tests

In Figure 19, which are snapshots from a movie, it is possible to see how the fluorescent dye that is injected together with ethanol is spreading in the microchannels, proving that they in fact are hollow. However the flow rate in the channels is slow when comparing to the theoretical flow rate of 2 mm/s. Ethanol was used because it is easier to inject than water due to its lower surface tension. The highest pressure applied was around 50 mbar and it seems likely that the  $\text{Al}_2\text{O}_3$  wall can withstand that pressure since no leakage was observed from the channels. Leakage was observed from structures that had collapsed around the channels already during the wet etch as can be seen in Figure 20.

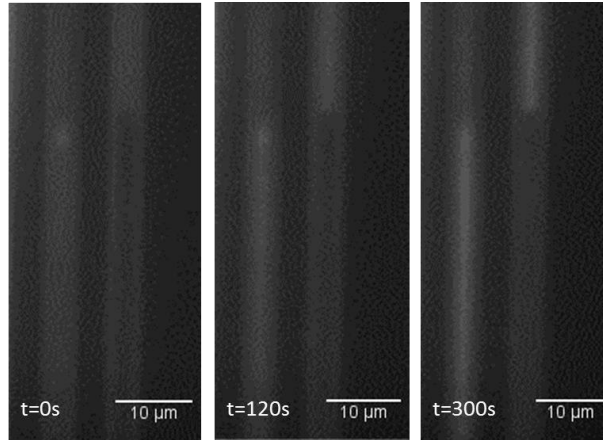


Figure 19. Fluorescent dye spreading in microchannels of  $\text{Al}_2\text{O}_3$  after an applied pressure of 50 mbar.

When the fluid in the channels had stopped moving a syringe was connected to the outlet and the fluid was manually forced through the system. The spreading in the channels before and after can be seen in Figure 20. It is also possible to see that the dye is leaking from the left channel as was expected since the structure had collapsed during aqua regia etch. The channel in the middle still transports the fluids though and appears to not be leaking.

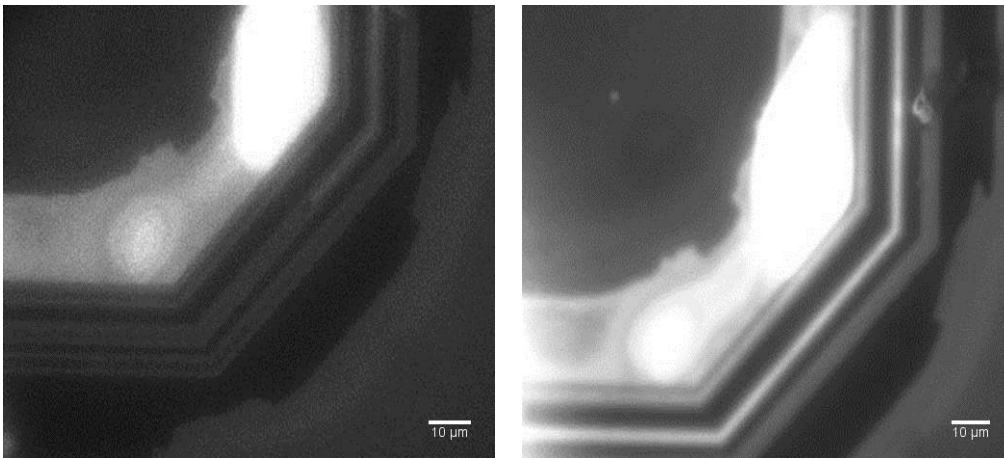


Figure 20. The collapsed structure outside the channels accumulates fluorescent dye that leaks from the left channel. The channel in the middle remains intact and the dye is transported.

### 5.3 COMSOL

The COMSOL modeling aided in the understanding of the fluid spreading and mixing in the channels. Since the flow is laminar in these small channels, a suggestion for the new design was that all bays and edges should be removed since they will delay the mixing time of the injected fluids and the true concentration can be difficult to find out. The top two images in Figure 21 shows one of the channels from the design that has been used mostly throughout this project and the two bottom ones a new proposed design.

In the model, a pressure of 10 kPa is applied to all three inlets and a concentration of  $1\text{mol/m}^3$  is injected at time,  $t=0.2\text{ s}$ . The two snapshots are from  $t=0.5\text{ s}$  and  $t=1\text{ s}$  and the different colors indicate how the concentration is changing along the channel. As can be seen, the test channel has a gradient in the concentration throughout the chamber and the mixing is never complete due to the different lengths of the inlets (cannot be seen in the zoomed in image) and the sharp edges in the chamber. The same model is used to simulate the flow in the new design and as seen, the mixing is complete much faster.

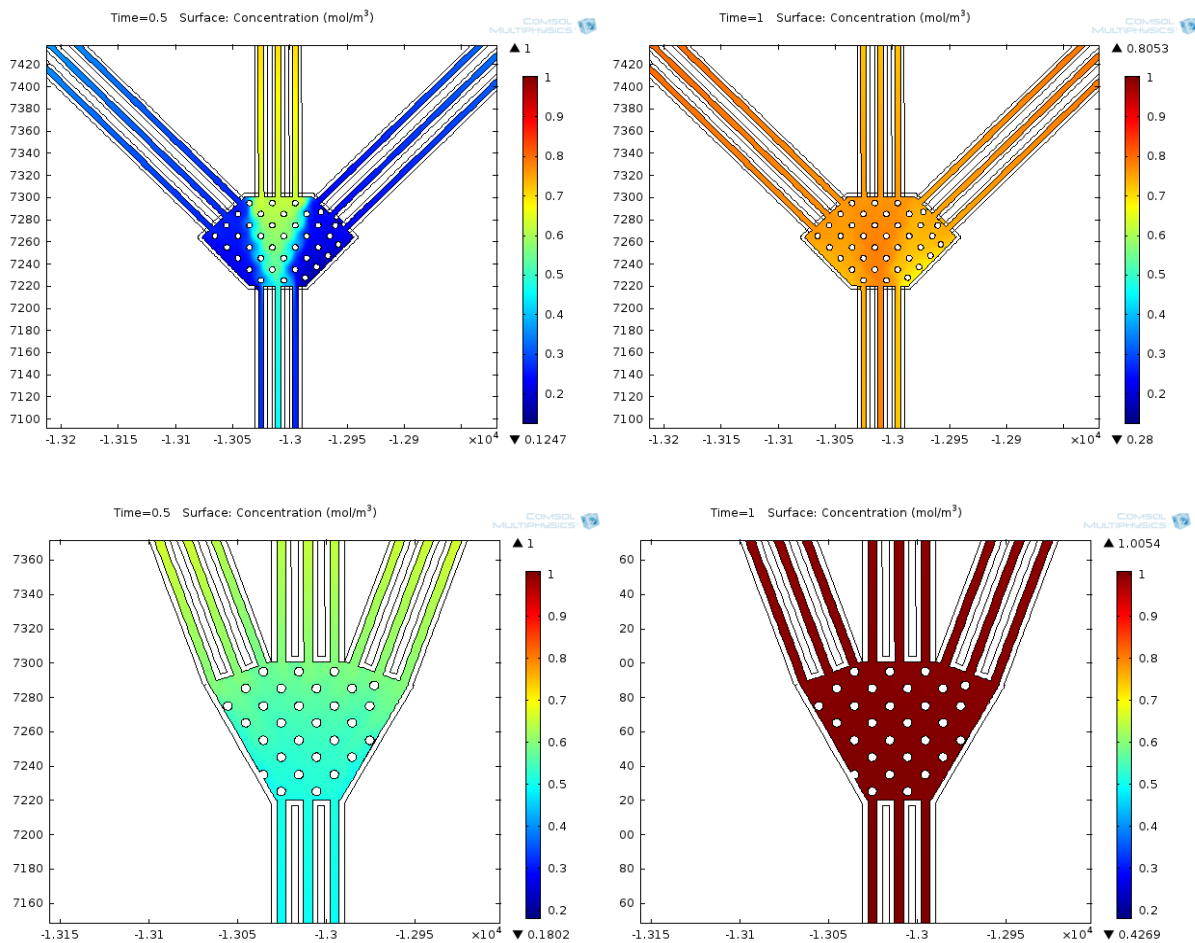


Figure 21. The two top pictures shows modeling of the real test structure that was used to fabricate the device while the two bottom ones shows how the design could be improved to obtain a homogenous mixture in the chamber where the NWs should be positioned.

## 6 Discussion

The fabrication of the fluidic device has been adapted in all steps to also function with nanowires with insight from earlier experience, basic experiments and literature. This gives great promise for the future fabrication tests where hollow nanowires will be created on top of the channels. Due to its hardness  $\text{Al}_2\text{O}_3$  has been chosen as final material of the nanoinjection needles as it should be able to withstand the stress during fabrication and the shear expected due to the motion of fluid and cells. It is also biocompatible and has previously shown to be suitable for the creation of hollow nanowires in cell injection experiments.

The device dimensions can be varied by changing some of the process steps, e.g. the channel width can be changed just by changing some of the lithography parameters. The width of the inner diameter of the needles might be adjusted by varying the ZnO layer deposited on the wires after growth. This means that the diameter could be changed if needed after results on cell viability have been obtained, since different diameters of the wires can change if the cells are resting on the nanowires or being pierced by them. The length of the needles can also be adjusted by etching the BCB layer and thus changing the protruding portion the NWs. In this way the fabrication alone could be tuned to optimize the device performance without the need to change the NW growth parameters.

A future device based on our work would enable sequential and controlled injection of molecules into cells that would allow one to study repeated exposure. The fact that fluids could be pushed through the channels with greater control and speed than diffusion means that investigating the immediate cell response such as ATP production, protein regulation and mitosis, to a given set of reagent would be possible opening up for novel types of interesting applications. It also puts much fewer limitations on the type of molecules that can be injected into the cells since they do not have to be loaded within a cargo or attached to needles that requires conjugated functional groups.

## 7 Conclusion

This project has showed the possibility to create microchannels in  $\text{Al}_2\text{O}_3$  starting from a III-V substrate and the tests carried out with NWs indicate that it would be possible to integrate them in the process.

The results obtained from the fabrication and device testing, together with the COMSOL modeling, was used by QuNano AB in the development of a new design for the nanoinjection devices. Information of what dimensions of the channels are suitable as well as how to minimize the risk of channel leakage was considered in the new design. From tests with NWs it was found that there is a large risk of the NWs being cross-linked in negative resist and break while etching  $\text{Al}_2\text{O}_3$ . This was not the case with positive PR, which is important knowledge in creating masks for UV-lithography. It was also found that wolfram serves well as an etch mask even for the wires during the InAs etch, which would otherwise have demanded a new process. One of the most important conclusion from the tests was that the channels could be supported by BCB and thus that all InAs could be removed from the rest of the sample, since the leakage of wet etchant into the supporting InAs layer was one of the main problems during this project.

By combining the fabrication steps that have been outlined during this project with the process to create HNWs, as was carried out by Persson et. al. [1], the prospects of reaching a nanoinjection needle device with pressure driven flow are significantly improved for cell injection experiments.

## 8 Summary

A microfluidic device has been fabricated from a test design proposed by QuNano AB. All of the results from the process steps together with modeling have aided in a new design for the chips. Some basic tests were also conducted on semiconductor nanowires to ensure they could be integrated in the process, since the aim of the final device is for it to be used as a nanoinjection needle in cell injection experiments, where the channels are to be used to transport the injection molecules. The project was carried out in the biophysics group at the division of Solid State Physics, Lund University and in cooperation with QuNano AB.



## 9 References

- [1] H. Persson, J. P. Beech, L. Samuelson, S. Oredsson, C. N. Prinz and J. O. Tegenfeldt, "Vertical oxide nanotubes connected by subsurface microchannels," *Nano Res.*, vol. 5, no. 3, pp. 190-198, 2012.
- [2] P. D. Robbins and S. C. Ghivizzania, "Viral Vectors for Gene Therapy," *Pharmacol. Ther.*, vol. 8, no. 1, pp. 35-47, 1998.
- [3] D. J. Stephens and R. Pepperkok, "The many ways to cross the plasma membrane," *Proceedings of the National Academy of Sciences of the USA*, vol. 98, no. 8, pp. 4295-4298, 2001.
- [4] T. M. Klein and S. Fitzpatrick-Mcelligottb, "Particle bombardment: a universal approach for gene transfer to cells and tissues," *Current Opinion in Biotechnology*, vol. 4, no. 5, pp. 583--590, 1993.
- [5] Y. C. Lin and M. Y. Huang, "Electroporation microchips for in vitro gene transfection.," *Journal of Micromechanics and Microengineering*, vol. 11, pp. 542-547, 2001.
- [6] J. C. Weaver, "Electroporation of cells and tissues," *IEEE Transactions on Plasma Science*, vol. 28, no. 1, pp. 24-33, 2000.
- [7] Y. Zhang och L.-C. Yu, "Microinjection as a tool of mechanical delivery," *Current Opinion in Biotechnology*, vol. 19, pp. 506-510, 2008.
- [8] T. E. McKnight, A. V. Melechko, G. D. Griffin, M. A. Guillorn, V. I. Merkulov, F. Francisco Serna, D. K. Hensley, M. J. Doktycz, D. H. Lowndes och M. L. Simpson, "Intracellular integration of synthetic nanostructures with viable cells for controlled biochemical manipulation," *Nanotechnology*, vol. 14, pp. 551-556, 2003.
- [9] N. Sköld, W. Hällström, H. Persson, L. Montelius, M. Kanje, L. Samuelson, C. N. Prinz and J. O. Tegenfeldt, "Nanofluidics in hollow nanowires," *Nanotechnology*, vol. 21, no. 15, p. 155301, 2010.
- [10] J. J. VanDersarl, A. M. Xu and N. A. Melosh, "Nanostraws for Direct Fluidic Intracellular Access," *Nano Letters*, vol. 12, no. 8, pp. 3881-3886, 2012.
- [11] E. Peer, A. Artzy-Schnirman, L. Gepstein and U. Sivan, "Hollow nanoneedle array and its utilization for repeated administration of biomolecules to the same cells," *ACS Nano*, vol. 6, no. 6, pp. 4940-4946, 2012.
- [12] T. M. Squires and Q. S. R, "Microfluidics: fluid physics at the nanoliter scale," *Reviews of Modern Physics*, vol. 27, pp. 997-1026, 2005.
- [13] L. Samuelson, C. Thelander, M. T. Björk, M. Borgströma, K. Deppert, K. A. Dick, A. E. Hansena, T. Mårtenssona, N. Paneva, A. I. Persson, W. Seiferta, N. N. Sköld, M. W. Larsson and L. R. Wallenberg, "Semiconductor nanowires for 0D and 1D physics and applications," *Physica E: Low-dimensional Systems and Nanostructures*, vol. 5, no. 2-3, pp. 313-318, 2004.

- [14] K. A. Dick, K. Deppert, L. Samuelson and W. Seifert, "InAs nanowires grown by MOVPE," *Journal of Crystal Growth*, vol. 298, pp. 631-634, 2007.
- [15] S. Sze, *Semiconductor Devices: Physics and Technology*, 2nd ed., Toronto: Wiley, 1985.
- [16] T. Mårtensson, M. Borgström, W. Seifert, B. J. Ohlsson and L. Samuelson, "Fabrication of individually seeded nanowire arrays by vapour–liquid–solid growth," *Nanotechnology*, vol. 14, p. 1255, 2003.
- [17] R. Puurunen, "Surface chemistry of atomic layer deposition: A case study for the trimethylaluminum/water process," *Journal of Applied Physics*, vol. 97, p. 121301, 2005.
- [18] J. Elam and S. George, "Growth of ZnO/Al<sub>2</sub>O<sub>3</sub> Alloy Films Using Atomic Layer Deposition Techniques," *Chemistry of Materials*, vol. 15, pp. 1020-1028, 2003.
- [19] B. Window, "Recent advances in sputter deposition, Surface and Coatings Technology," *Surface and Coatings Technology*, vol. 71, pp. 93-97, 1995.
- [20] D. M. Mattiox, *Handbook of Physical Vapor Deposition (PVD) Processing (Second Edition)*, Park Ridge, NJ: Noyes Publication, 2010.
- [21] Y. Xia and G. M. Whitesides, "Soft Litography," *Annual Review of Materials Science*, vol. 28, pp. 153-184, 1998.
- [22] M. A. Eddings, M. A. Johnson and B. K. Gale, "Determining the optimal PDMS–PDMS bonding technique for microfluidic devices," *Journal of Micromechanics and Microengineering*, vol. 18, no. 6, 2008.
- [23] R. Reichelt, "Scanning Electron Microscopy," in *Science of Microscopy*, New York, Springer, 2007, pp. 133-272.
- [24] G. Binnig, "Force Microscopy," *Ultramicroscopy*, Vols. 42-44, no. 1, pp. 7-15, 1992.
- [25] J. W. Lichtman and J.-A. Conchello, "Fluorescence microscopy," *Nature Methods*, vol. 2, no. 12, pp. 910-919, 2005.
- [26] F. N. Dultsev and V. G. Kesler, "Etching and oxidation of InAs in planar inductively coupled plasma," *Applied Surface Science*, vol. 256, pp. 246-250, 2009.
- [27] B. T. Lee, T. R. Hayes, P. M. Thomas, R. Pawelek och P. F. Sciortino Jr, "SiO<sub>2</sub> mask erosion and sidewall composition during CH<sub>4</sub>/H<sub>2</sub> reactive ion etching of InGaAsP/InP," *Applied Physics Letter*, vol. 63, p. 3170, 1993.

# Development and Fabrication of a Microfluidic Device for Future Applications in Cell Injection Experiments

Susanne Norlén<sup>1</sup>, Henrik Persson<sup>1</sup>, Truls Löwgren<sup>2</sup> & Jonas Tegenfeldt<sup>1,3</sup>

<sup>1</sup>Division of Solid State Physics, Lund University

<sup>2</sup>QuNano AB

<sup>3</sup> Department of Physics, University of Gothenburg

## Abstract

Injection of molecules into cells is used in life sciences and biology today to study cell response to certain substances. Delivery of controlled amounts is important for single cell injection experiments and furthermore, the technique needs to be noninvasive which can be hard with today's micropipettes. The growing field of nanotechnology has interested many researchers for this purpose and several groups are focusing on developing injection tools with dimensions at the nanoscale. So far the developed techniques have been limited either to single injections or by the slow process of diffusion which are barriers that needs to be overcome in this area. Our solution is to develop a microfluidic device with hollow nanowires (HNWs) that has the ability to inject molecules into cells with a pressure driven flow, since this could allow fast and repeated injection of substances. Therefore, a microfluidic system has been created, as first step in the development of such a device. The channel walls are made of atomic layer deposited  $\text{Al}_2\text{O}_3$  and supported by a cured benzocyclobutene based resin. The fabrication of the channels has been realized by etching down microstructures in an epitaxially grown InAs substrate. The fact that the fabrication starts from a III-V substrate opens up the possibility to integrate semiconductor nanowires (NWs) in the process in the future, since they can be epitaxially grown on III-V substrates. The wires can be used as templates for creating injection needles with nanodimensions. The functionality of the channels has been proven in fluidic tests where a fluorescent dye was injected with an applied pressure of around 50 mbar. In the future, when nanowires are connected to the channels, cells could be cultured on top of the wires and substances introduced through the fluidic system to reach the cells. This means that faster injection than similar devices that rely on diffusion through the system could be realized with a method that allows for repeated and controlled injection of molecules.

**Keywords:** Hollow nanowires, cell injections, III-V material, dry etch, wet etch

## 1. Introduction

Injection of molecules into single cells can be carried out with microneedle injection, but since the pipettes are in the same size range as the cells there is a risk of cells rupturing during injection. Therefore, several research groups are now exploring the potential use of injection needles with dimensions at the nanoscale since they, due to their small size, are less invasive. E.g. McKnight et al. [1] have delivered plasmid DNA into cells by attaching it onto carbon nanofibers which allowed cultured cells on top of the fibers to express the gene supplied. The same principle was also used by Shalek et al. who attached molecules onto silicon nanowires [2]. The drawbacks of this technique are that multiple injections are not possible and there are limits to what type of molecules that can be attached to the fibers.

Another approach has been to create hollow structures through which molecules can diffuse. VanDersarl et al. [3] created their “nanostraws” by etching down alumina coated nanopores and through a channel underneath, molecules could diffuse through the straws into cells that had been pierced by them. In this way they successfully injected green fluorescent protein (GFP) into cells. Peer et al. [4] also showed repeated injections of molecules into cells through nanoneedles without any long-term effect on the wellbeing of the cells and without transfecting nearby cells that were not in contact with the needles. The molecules diffused from a reservoir on the back of the chip and the fluid could easily be switched to inject other substances into the cells. The methods described above are either restricted by the slow process of diffusion or limited to single injections only and fast and serial injections of molecules into cells still remains a problem.

To address this limitation of current techniques we have developed a channel system of a microfluidic device that can be connected to a macroscopic fluidic control system. The fabrication starts from an InAs buffer substrate which opens up the possibility to connect the channels to hollow nanotubes in the future. This would enable injection of molecules into cells with a pressure driven flow instead of diffusion and the fabrication of the hollow oxide tubes can be adopted from Persson et al. [5] by using nanowires as templates. The device functionality is illustrated in Figure 1.

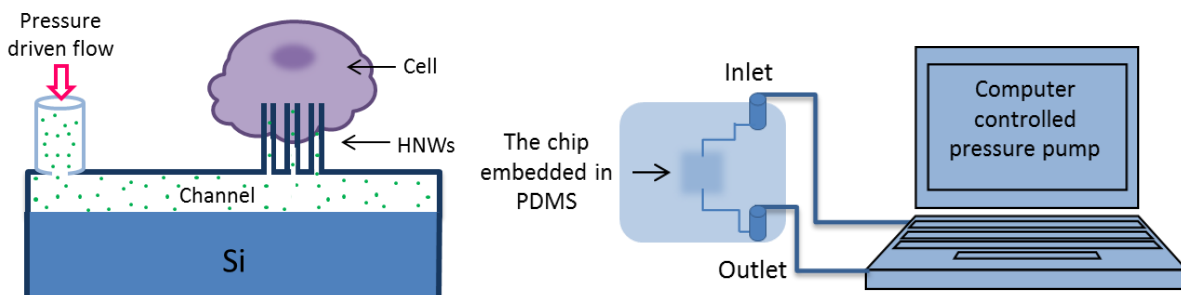


Figure 1. Illustrations of the final device and its functionality, Note that the illustrations are not drawn to scale.

## 2. Fabrication Method

### 2.1 Creation of microchannels

The process to fabricate the channels is drawn schematically in Figure 2. The nanowires are in the pictures to illustrate their positions, even though this work has focused on creating the channel system. The channels are 5  $\mu\text{m}$  wide and 2 mm long.

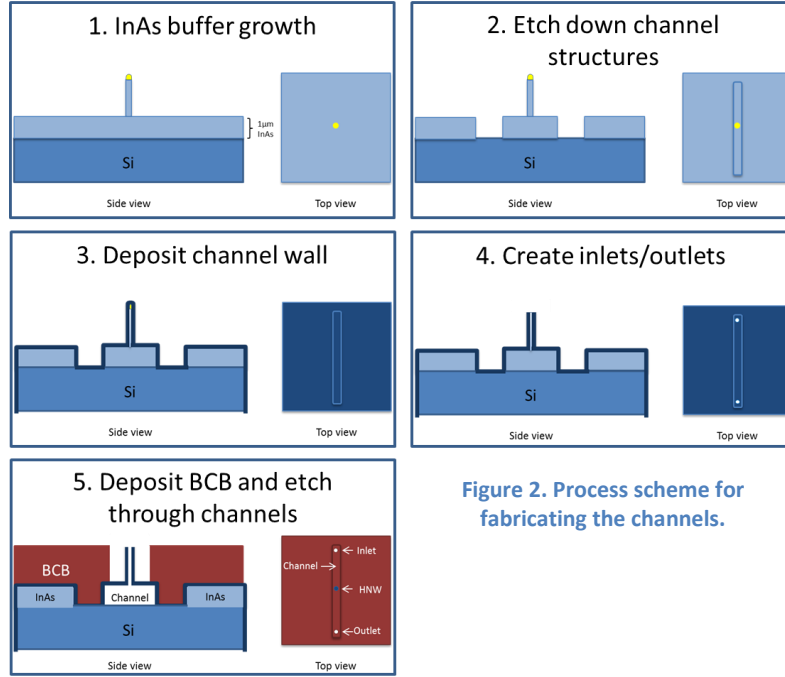


Figure 2. Process scheme for fabricating the channels.

An InAs buffer was epitaxially grown with metal organic vapor phase epitaxy (MOVPE), which can also be used to grow InAs nanowires [6]. The equipment was from Aixtron and the precursors used were TMIn and AsH<sub>3</sub>. When nanowires are integrated in the process, these can be positioned with electron beam lithography (EBL) defined growth sites [7].

The InAs buffer was patterned using UV-lithography in channel-like structures and the area surrounding the channels was etched down all the way to the Si substrate. Dry etch of InAs was carried out using inductively coupled plasma reactive ion etch (ICP RIE) with CH<sub>4</sub>/Ar/H<sub>2</sub> chemistry as have been previously described [8]. A hard mask of wolfram was used to obtain vertical etch walls in the end, even though other materials such as silicon dioxide and chromium have been tested as well.

To create the actual oxide wall a layer of 1000 cycles Al<sub>2</sub>O<sub>3</sub> was deposited on the samples with atomic layer deposition (ALD). The precursors trimethylaluminum (TMAI) and H<sub>2</sub>O were alternatingly introduced into the chamber, building a conformal layer that completely covers all structures on the sample. We used 1000 cycles to create a channel wall with a thickness of ~100 nm.

Channel inlets and outlets were formed by opening up holes in the Al<sub>2</sub>O<sub>3</sub> in each end of the channels. The holes were patterned with UV-lithography and etched in CF<sub>4</sub>/H<sub>2</sub> chemistry using ICP

RIE. Dry etch was preferred not to risk damaging the  $\text{Al}_2\text{O}_3$  of the channel wall in case wet etchant would spread.

To create freestanding channels, the InAs under the  $\text{Al}_2\text{O}_3$  in the channels needs to be removed. This was achieved by immersing the samples in aqua regia ( $\text{HCl}:\text{HNO}_3$ , 3:1). To protect the front of the sample from the etchant, a layer of a benzocyclobutene based resin (BCB 3022-46, DOW Chemical) was spin coated onto the samples and cured in a  $\text{N}_2$  environment prior to the etch step.

As a final step in the fabrication process a patterned piece of polydimethylsiloxane (PDMS) was attached on the front of the sample to function as a link between the device and the pressure pump. The liquid, uncured PDMS was first mixed with a catalyst at a ratio of 1:10 and molded on a SU8-master with soft lithography. In this way channels that match the in- and outlets on the samples were created in the polymer. The pieces were bonded together by exposing them to a 60s  $\text{O}_2$  plasma which is frequently used to bond PDMS for microfluidic applications [9].

## 2.2 Fluidic tests

To test the functionality of the channels, ethanol mixed with a fluorescent dye was injected through the PDMS structures and eventually reaching the  $\text{Al}_2\text{O}_3$  channels on the device. A pressure difference across the device,  $\Delta p$ , ranging from 0 to 50 mbar were applied and the movement of the dye was studied in an optical microscope.

The pressure-driven flow (Poiseuilles flow) in the channels gives a theoretical velocity,  $v$ , by [10]

$$v \sim \frac{\Delta p w^2}{\eta l} \quad [\text{Equation 1}]$$

Where  $w$  is the radius of a circular channel,  $\eta$  is the viscosity of the fluid and  $l$  is the length of the channel. By using the channel length of 2 mm and approximating the channels to be circular with a radius of 1  $\mu\text{m}$  a theoretical velocity of 2 mm/s is obtained. This was calculated by using the viscosity for ethanol of 1.22 mPas at  $T=293$  K.

## 3. Results

A fabrication scheme has been created to fabricate hollow oxide channels supported by a BCB membrane. Tests have also been conducted on samples with nanowires to ensure that they can be integrated in the process in the future.

### 3.1 Fluidic device

In Figure 3 one can see two scanning electron microscope (SEM) images of the channels after patterning and the dry etch of InAs. The left image shows three parallel channels before oxide deposition. The right picture shows how smooth, vertical etch walls are obtained by using wolfram as a mask during the dry etch. The etched down area is free from residues which is important to prevent channel leakage.

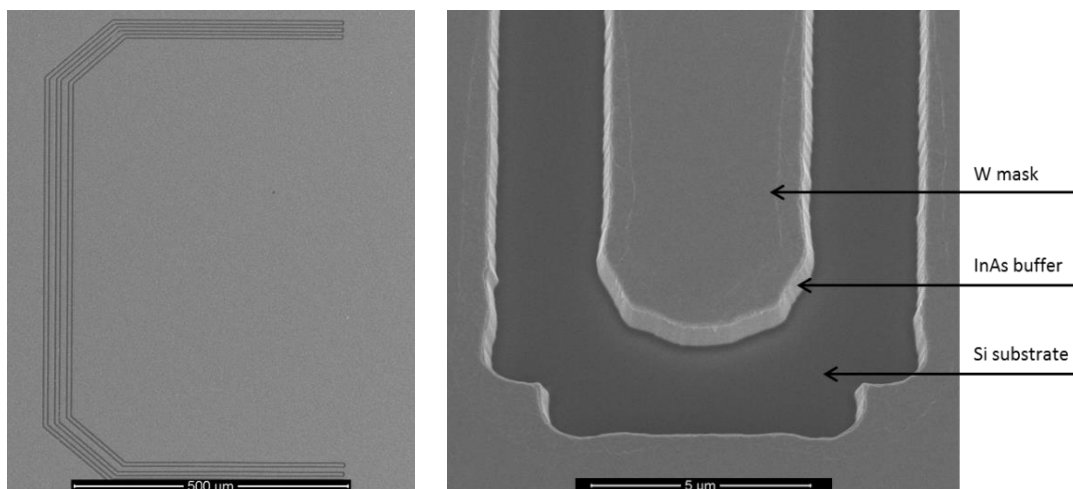


Figure 3. Left: Three parallel channels after the InAs have been etched down on the sides. Right: A zoomed in SEM image of the end of a channel where vertical walls have been obtained by using W as an etch mask during InAs dry etch.

In Figure 4 it is possible to see how the etchant is removing InAs in the narrow oxide channels. Since the channels are extremely narrow (5 μm wide) the etch rate is slow (~1 μm/min). The etch rate is also decreasing further into the channels due to the limited diffusion of etchant in and products out of the structures.

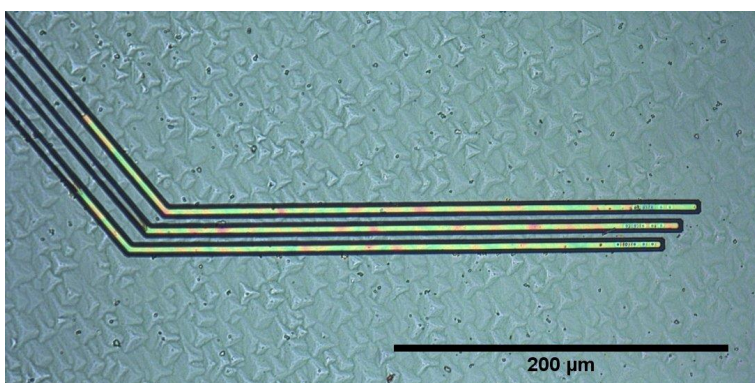


Figure 4. The spreading of aqua regia in microchannels of  $\text{Al}_2\text{O}_3$ .

The BCB layer (not on the sample in Figure 4) helps to stabilize the channels during the acid etch and also prevents etchant to reach other structures on the sample, which could cause damage to the channels.

### 3.2 Fluidic tests

In Figure 5, which shows snapshots from a movie, it is possible to see how the fluorescent dye that is injected together with ethanol is spreading in the microchannels, proving that they in fact are hollow.

However, the flow rate in the channels is slow when comparing to the theoretical flow rate of 2 mm/s. We used ethanol because it is easier to inject than water due to its lower surface tension. The highest pressure applied on the PDMS channel was around 50 mbar which is the pressure that is divided over the three  $\text{Al}_2\text{O}_3$  channels. It shows that the  $\text{Al}_2\text{O}_3$  wall can withstand that pressure in that range when supported by BCB, since no leakage was observed from the channels.

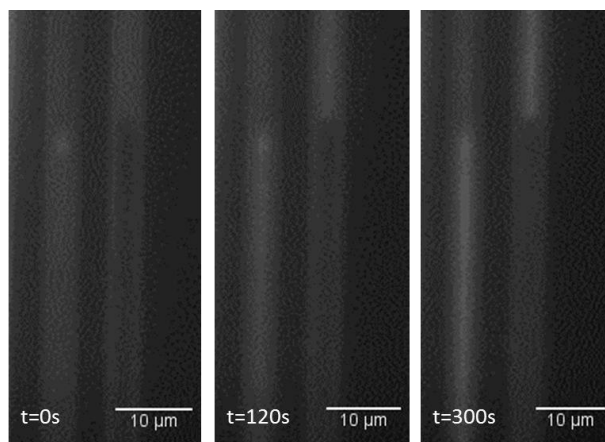


Figure 5. Fluorescent dye spreading in microchannels.

#### 4. Discussion

The fabrication of the fluidic device has in all steps been adapted to also function with nanowires. This gives great promises for future implementation of devices where hollow nanowires will be created on top of the channels. Due to its hardness  $\text{Al}_2\text{O}_3$  has been chosen as final material of the injection needles as it should be able to withstand the stress during fabrication. It is also biocompatible and has previously shown to be suitable for the creation of hollow nanowires in cell injection experiments.

A future device based on our work would enable sequential and controlled injection of molecules into cells that would allow one to study repeated exposure. The fact that fluids could be pushed through the channels with greater control and speed than diffusion means that investigating the immediate cell response such as ATP production, protein regulation and mitosis, to a given set of reagent would be possible opening up for novel types of interesting applications. It also puts much fewer limitations on the type of molecules that can be injected into the cells since they do not have to be loaded within a cargo or attached to needles that requires conjugated functional groups.

#### 5. Conclusion

We have shown that it is possible to fabricate hollow microchannels in  $\text{Al}_2\text{O}_3$  starting from a III-V substrate. The fluidic tests on the channel system has shown that transport through these narrow channels with a pressure driven flow is possible. The tests that have been carried out with NWs has outlined a fabrication scheme for integrating these in the process and this holds great promise for developing this device further for use in cell injection experiments.



## 6. References

- [1] T. E. McKnight, A. V. Melechko, G. D. Griffin, M. A. Guillorn, V. I. Merkulov, F. Francisco Serna, D. K. Hensley, M. J. Doktycz, D. H. Lowndes och M. L. Simpson, "Intracellular integration of synthetic nanostructures with viable cells for controlled biochemical manipulation," *Nanotechnology*, vol. 14, pp. 551-556, 2003.
- [2] A. K. Shalek, J. T. Robinson, E. S. Karp, J. S. Lee, D.-R. Ahn, M.-H. Yoon, A. Sutton, M. Jorgolli, R. S. Gertner, T. S. Gujral, G. MacBeath, E. G. Yang och H. Park, "Vertical silicon nanowires as a universal platform for delivering biomolecules into living cells," *Proceedings of the National Academy of Sciences of the USA*, vol. 107, nr 5, pp. 1870-1875, 2010.
- [3] J. J. VanDersarl, A. M. Xu and N. A. Melosh, "Nanostraws for Direct Fluidic Intracellular Access," *Nano Letters*, vol. 12, no. 8, pp. 3881-3886, 2012.
- [4] E. Peer, A. Artzy-Schnirman, L. Gepstein and U. Sivan, "Hollow nanoneedle array and its utilization for repeated administration of biomolecules to the same cells," *ACS Nano*, vol. 6, no. 6, pp. 4940-4946, 2012.
- [5] H. Persson, J. P. Beech, L. Samuelson, S. Oredsson, C. N. Prinz and J. O. Tegenfeldt, "Vertical oxide nanotubes connected by subsurface microchannels," *Nano Res.*, vol. 5, no. 3, pp. 190-198, 2012.
- [6] K. A. Dick, K. Deppert, L. Samuelson and W. Seifert, "InAs nanowires grown by MOVPE," *Journal of Crystal Growth*, vol. 298, pp. 631-634, 2007.
- [7] T. Mårtensson, M. Borgström, W. Seifert, B. J. Ohlsson and L. Samuelson, "Fabrication of individually seeded nanowire arrays by vapour-liquid-solid growth," *Nanotechnology*, vol. 14, p. 1255, 2003.
- [8] F. N. Dultsev and V. G. Kesler, "Etching and oxidation of InAs in planar inductively coupled plasma," *Applied Surface Science*, vol. 256, pp. 246-250, 2009.
- [9] M. A. Eddings, M. A. Johnson and B. K. Gale, "Determining the optimal PDMS-PDMS bonding technique for microfluidic devices," *Journal of Micromechanics and Microengineering*, vol. 18, no. 6, 2008.
- [10] T. M. Squires and Q. S. R, "Microfluidics: fluid physics at the nanoliter scale," *Reviews of Modern Physics*, vol. 27, pp. 997-1026, 2005.